ISOMETRIC IMMERSIONS WITH RECTIFIABLE GEODESICS

QING HAN, MARTA LEWICKA AND L. MAHADEVAN

Abstract. Kirigami is the art of cutting paper to make it articulated and deployable, allowing for it to be shaped into complex two and three-dimensional geometries. The mechanical response of a kirigami sheet when it is pulled at its ends is enabled and limited by the presence of cuts that serve to guide the possible non-planar deformations. Inspired by the geometry of this art form, we ask two questions: (i) What is the shortest path between points at which forces are applied? (ii) What is the nature of the ultimate shape of the sheet when it is strongly stretched? Mathematically, these questions are related to the nature and form of geodesics in the Euclidean plane with linear obstructions (cuts), and the nature and form of isometric immersions of the sheet with cuts when it can be folded on itself, and are related to a class of questions associated with isometric immersions in differential geometry and geodesics in discrete and computational geometry. We provide a constructive proof that the geodesic connecting any two points in the plane is piecewise polygonal. We then prove that the family of polygonal geodesics can be simultaneously rectified into a straight line by flat-folding the sheet so that its configuration is a (non-unique) piecewise affine planar isometric immersion.

1. Introduction

A thin rectangular sheet of paper pulled at its corners is almost impossible to stretch. Introducing a cut in its interior changes its topology, and thence changes its physical response. The corners can now be pulled apart as the sheet bends out of the plane, see Figure 1.1. The physical reason for this is that the geometric scale-separation associated with a sheet of thickness h and size L (where $h \ll L$), makes it energetically expensive to stretch and easy to bend, since the elastic potential energy of the sheet per unit area can be written as:

$$\mathcal{E} = Eh(\text{stretching strain})^2 + Eh^3(\text{curvature})^2, \tag{1.1}$$

where the *stretching strain* and *curvature* characterize the modes of deformation of the sheet, and E is the elastic modulus of the material. Thus, as $h/L \to 0$, for given boundary conditions it is energetically cheaper to deform by bending (curving) rather than stretching, as can be observed readily with any thin sheet of any material. This observation and its generalizations are behind the Sino-Japanese art of kirigami (kiri = cut, gami = paper).

Motivation from solid mechanics. Recently, this ability to make cuts in a sheet of paper that allow it to be articulated and deployed into complex two and three-dimensional patterns, has become the inspiration for a new class of mechanical metamaterials [3, 1]. The geometrical and topological properties of the slender sheet-like structures, irrespective of their material constituents, can then be exploited to create functional structures on scales ranging from the nanometric [2] to centimetric and beyond [20, 15, 16]. Of the various mathematical and physical questions that arise from this ability to control the configurational degrees of freedom of the sheet using the geometry and topology of the cuts, perhaps the simplest is the following: if a sheet with random cuts was pulled at two points on the boundary, what is the nature of paths of stress transmission through the sheet?

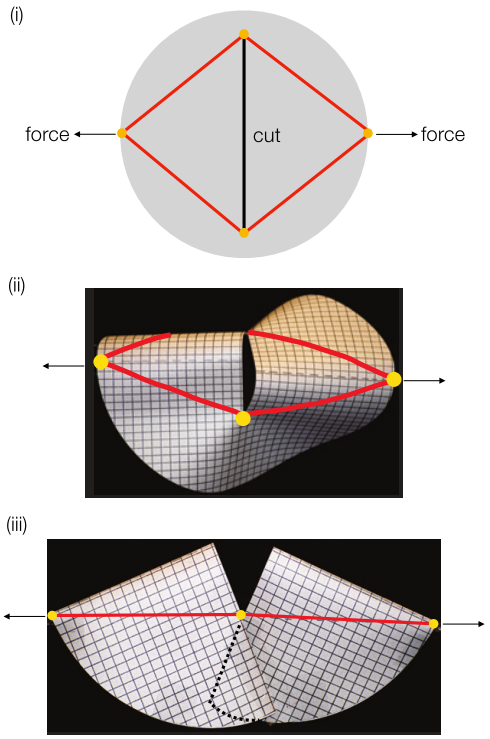

FIGURE 1.1. A circular sheet of paper with a cut in it becomes soft, because the cut allows the sheet to buckle out of the plane when pulled by two equal and opposite forces at its boundary. (i) The red lines are the geodesics connecting the points of force application. (ii) As the sheet deforms, it creates conical structures that allow the sheet to deform further, thus causing the geodesics to straighten out. (iii) The ultimate shape of the sheet in the strongly deformed limit causes each polygonal geodesic to straighten out and yields a flat-folded sheet that is piecewise affine isometric to the plane, accompanied by set of sharp folds. [We thank G. Chaudhary for the photographs.]

In the absence of cuts, the lines of force transmission are straight lines connecting the points, i.e. geodesics, but this needs to be revisited in the presence of obstructing cuts. One might ask about the nature of the paths of force transmission, i.e. the geodesics, in this situation. The results of qualitative experiments with a sheet of paper that has a single cut along the perpendicular bisector to the line joining the points of force application, are shown in Figure 1.1. For small forces, the sheet deforms into two conical regions that allow the edge of the cut to curve out of the plane, and when the forces are large enough, the ends of the cut become approximately collinear with the line joining the points of forcing. Observations of sheets with multiple cuts are suggestive of a generalization, namely that cuts cause the sheet to buckle out of the plane until a straight geodesic in $\mathbb{R}^3$ connects the points of force application. Furthermore, as the sheet thickness becomes vanishingly small, allowing the sheet to form sharp creases with a large curvature, the sheet can fold on itself and become flat again, as seen in Figure 1.1 (iii).

Motivation from differential geometry. The observations of the sheet folding on itself is of course reminiscent of a class of famous problems in mathematics, that of isometric immersions and embeddings of manifolds of a lower dimension in one of a higher dimension. In a remarkable paper published more than half a century ago, Nash [19] proved that any smooth n-dimensional Riemannian manifold admits a (global) smooth isometric embedding in some Euclidean space $\mathbb{R}^N$, for some large dimension $N = N(n) > n$. The techniques involving smoothing operators introduced by Nash to resolve the loss of derivatives were modified by many people, and led to what is now known as the hard implicit function theorem, or the Nash-Moser-Hörmander iteration. Complementing this, others

such as Günther [13] vastly simplified Nash's proof and improved the dimension N; for for a historical account of the smooth isometric embeddings and relevant results, see [14].

On the one hand, many problems are still open concerning the smallest possible dimension N. What is the smallest N such that *any* smooth n-dimensional Riemannian manifold admits a smooth isometric embedding in the Euclidean space $\mathbb{R}^N$? For $N = n(n+1)/2$, the so-called Janet dimension, what are topological/geometrical obstructions for a smooth n-dimensional Riemannian manifold to admit a smooth isometric embedding in the Euclidean space $\mathbb{R}^N$?

On the other hand, the celebrated Nash-Kuiper theorem [17, 18] asserts that any C^1 short immersion or embedding from a compact n-dimensional manifold M with a C^1 metric into $\mathbb{R}^{n+1}$ can be uniformly approximated by C^1 isometric immersions or embeddings. Recently, this regularity has been improved by Conti, Delellis and Székelyhidi [4] to $C^{1,\theta}$ isometric immersions with any $\theta < \frac{1}{1+n+n^2}$. For the special case of the 2-dimensional disc $M = D^2$, where one can take advantge of the theory of conformal maps, De Lellis, Inauen, and Székelyhidi [6] proved that any C^1 short immersion of D^2 into $\mathbb{R}^3$ can be uniformly approximated by $C^{1,\theta}$ isometric immersions for any $\theta < 1/5$. The mentioned results at the optimal (so far) exponents both for general n and $n = 2$, were extended to isometric immersions and embeddings of compact manifolds in [5].

Results in this paper. Inspired by the physical experiments and the above links, in this paper we initiate a study of isometric immersions of (2-dimensional) surfaces in $\mathbb{R}^3$ from a new perspective. While isometric immersions of such surfaces are known to exist and, in fact, there are continuous families of isometric immersions, we aim to investigate the existence of isometric immersions with a nice characterization of geodesics connecting two given points. It is obvious that the geodesic (the shortest path) connecting two given points in three-dimensional Euclidean space is a line segment. This is not necessarily true for geodesics on two-dimensional surfaces in three-dimensional Euclidean spaces. In fact, geodesics on arbitrary two-dimensional smooth surfaces in three dimensional Euclidean space may not contain any line segments. For a given smooth two-dimensional surface in three-dimensional Euclidean space, if geodesics connecting two given points are not line segments, we ask whether we can deform the given surface isometrically to a new surface where these geodesics become a single line segment, i.e. the geodesic can be rectified into a straight line in three dimensions.

Finally, given the folded nature of the kirigamized paper, there is a third perspective on the problem, this time from the viewpoint of discrete and computational geometry [7] and the related subjects of mathematical and computational origami [8]. A natural question in these fields is that of finding shortest paths in an obstacle-ridden plane [9] or in polyhedral geometries and the related problems that typically lead to piecewise linear geodesics [10],[11]. However, to our knowledge, this literature while rich typically does not treat the case of multiply connected surfaces immersed in three dimensions that are also deformable into polyhedra with obstacles, the natural domain of physical and thus mathematical kirigami.

These different perspectives driven by the observations of the ultimate shape of a paper sheet with a cut in it, suggest two conjectures:

(i) geodesics in a planar sheet with cuts are piecewise linear, i.e. they are polygonals;
(ii) on pulling at two points in a sheet with cuts, these polygonal geodesics straighten out by allowing the sheet to deform in the third dimension, which when flat-folded causes the geodesic to be rectified, leading to a configuration that is a piecewise affine isometric immersion.

Here, we give rigorous proofs of the above two statements. As a final observation, we note that neglecting the bending and treating the stretching term as a constant, the energy minimization

problem for $\mathcal{E}$ in (1.1) reduces to minimizing the following simple energy:

$$\mathcal{E}_0(u) = -\big\langle F, u(p) - u(q)\big\rangle, \tag{1.2}$$

where by F is the load pulling the two points p and q of the sheet in opposite directions, and u is an isometric deformation of the sheet. Denoting by $\mathrm{dist}(p,q)$ the geodesic distance between p and q along curves that do not intesect the cuts, it is straighforward to see that:

$$\inf \mathcal{E}_0 \geq -|F| \cdot \sup |u(p) - u(q)| \geq -|F| \cdot \mathrm{dist}(p,q),$$

and that the minimum of $\mathcal{E}_0$ (if exists) is achieved for u taking the geodesics to a segment parallel to F. The main result of this paper shows that there indeed exists an isometric immersion which maps the geodesics into a straight line in $\mathbb{R}^3$. Consequently, it follows that:

$$\inf \mathcal{E}_0 = -|F| \cdot \mathrm{dist}(p,q).$$

Acknowledgement. M. Lewicka was partially supported by NSF grant DMS 2006439. L Mahadevan was partially supported by NSF grants BioMatter DMR 1922321 and MRSEC DMR 2011754 and EFRI 1830901.

2. The set-up and the main results of this paper

Let $\Omega \subset \mathbb{R}^2$ be a convex, bounded, planar domain and let L be the union of finitely many closed segments contained in Ω. We study the geodesic distance and the structure of geodesics in $\Omega \setminus L$.

Specifically, we work under the following setup:

(S) In an open, bounded, convex set $\Omega \subset \mathbb{R}^2$, given is a graph G, consisting of $\bar{n} \geq 2$ vertices $V = \{a_i\}_{i=1}^{\bar{n}}$ and $n \geq 1$ edges $E = \{l_i\}_{i=1}^{n}$, represented by:

$$l_i = \big\{(1-t)a_j + ta_k;\ t \in [0,1]\big\} \text{ for some } a_j \neq a_k \in V.$$

We denote $L = \bigcup_{i=1}^{n} l_i$ and call L the set of *cuts*. Without loss of generality, we further assume that G is a planar graph, i.e. for all $i \neq j$ the intersection $l_i \cap l_j$ is either empty or consists of a single point that is a common vertex of l_i and l_j.

The collection of cuts in L is thus finite but completely arbitrary, i.e. the cuts may have any length and orientation, and are allowed to intersect each other.

We next define:

(G) Given two points $p \neq q$ that belong to the same connected component of $\bar{\Omega} \setminus L$, we set:

$$\mathrm{dist}(p,q) = \inf\big\{\mathit{length}(\tau);\ \tau : [0,1] \to \bar{\Omega} \setminus L \text{ piecewise } \mathcal{C}^1 \text{ with } \tau(0) = p,\ \tau(1) = q\big\}.$$

Further, any piecewise $\mathcal{C}^1$ curve $\sigma : [0,1] \to \bar{\Omega}$ with $\sigma(0) = p$, $\sigma(1) = q$ is called a *geodesic from p to q in $\Omega \setminus L$*, provided that:

(i) $\mathit{length}(\sigma) = \mathrm{dist}(p,q)$,

(ii) σ is the uniform limit as $k \to \infty$, of a sequence of piecewise $\mathcal{C}^1$ curves $\{\tau_k : [0,1] \to \bar{\Omega} \setminus L\}_{k=1}^{\infty}$, each satisfying $\tau_k(0) = p$, $\tau_k(1) = q$.

The above definition abuses the notion of a geodesic slightly, because it allows σ to be not entirely contained in $\Omega \setminus L$ (although we call it a geodesic in $\Omega \setminus L$), that is, we allow cuts to be parts of σ. Figures 2.1 and 2.2 show a few examples of G, p, q and the resulting geodesics. Here and below, by $\overline{pa_{i_1}a_{i_2}\ldots a_{i_k}q}$ we denote the polygonal joining p and q through the consecutive points $a_{i_1}, a_{i_2}, \ldots, a_{i_k}$.

Our first result is as follows:

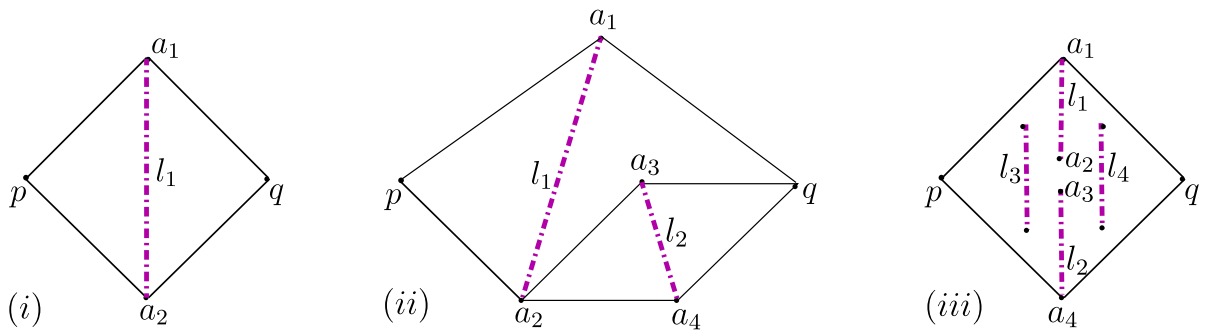

FIGURE 2.1. Three configurations of G, p, q with pairwise nonintersecting cuts: (i) $p = (0,-1), q = (1,0)$, $a_1 = (0,1), a_2 = (0,-1)$ yield two geodesics: $\sigma_1 = \overline{pa_1q}, \sigma_2 = \overline{pa_2q}$; (ii) $p = (0,0), q = (4,0)$, $a_1 = (2,(2^{3/2}-1)^{1/2}), a_2 = (1,-1), a_3 = (3,-1), a_4 = (4,0)$ yield three geodesics: $\sigma_1 = \overline{pa_1q}, \sigma_2 = \overline{pa_2a_3q}, \sigma_3 = \overline{pa_2a_4q}$; (iii) $p = (-1,0), q = (1,0)$, $a_1 = (0,1), a_4 = (0,-1)$ with $a_2, a_3 = (0, \pm\epsilon)$, $a_5, a_6, a_7, a_8 = (\pm\epsilon, \pm(1-\epsilon^{1/2}))$ for a sufficiently small $\epsilon > 0$ yield two geodesics: $\sigma_1 = \overline{pa_1q}, \sigma_2 = \overline{pa_4q}$.

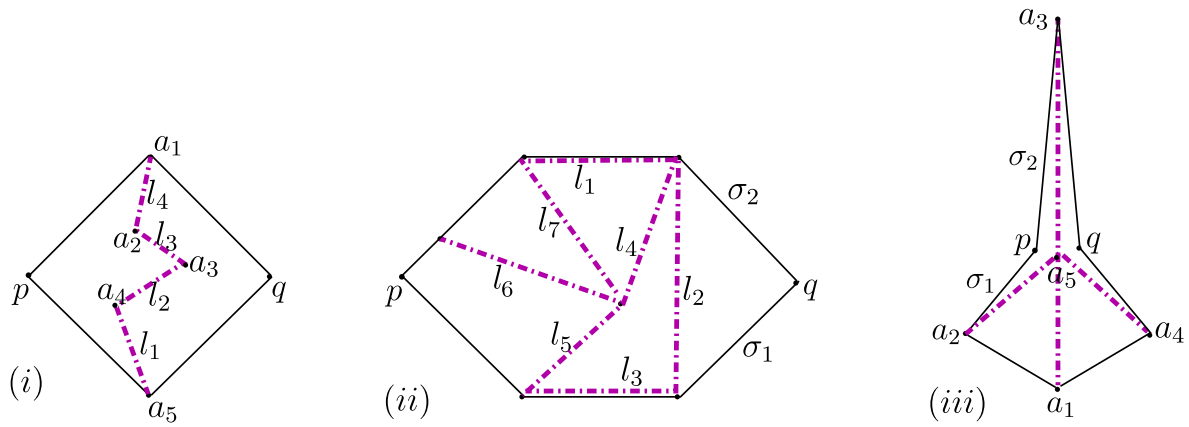

FIGURE 2.2. Three configurations of G, p, q with intersecting cuts: (i) $n = 4$, $\bar{n} = 5$ result in two geodesics: $\sigma_1 = \overline{pa_1q}, \sigma_2 = \overline{pa_5q}$, this configuration is minimal in the sense introduced in Section 4; (ii) $n = 7$, $\bar{n} = 6$ and two geodesics: σ_1, σ_2; (iii) $n = 4$, $\bar{n} = 5$ with $length(\overline{a_1a_2p}) = length(\overline{pa_3})$, this is also a minimal configuration resulting in two geodesics σ_1, σ_2.

Theorem 2.1. *Assume (S) and let $p, q \in \bar{\Omega} \setminus L$ belong to one connected component of $\bar{\Omega} \setminus L$. Then there exists at least one geodesic from p to q, as defined in (G). Each such geodesic σ satisfies:*

(i) σ is a finite polygonal joining p and q, with all its other vertices distinct and chosen from V,
(ii) for each $i = 1 \dots n$, if $\sigma \cap l_i \neq \emptyset$ then either $l_i \subset \sigma$ or $\sigma \cap l_i \subset \{a_j, a_k\}$, where $l_i = \overline{a_ja_k}$.

Our second result, the main contribution of this paper, is motivated by the general considerations in Section 1. We prove the existence of an isometric immersion of $\Omega \setminus L$ into $\mathbb{R}^3$, which bijectively maps each geodesic between two chosen boundary points p, q onto one segment in $\mathbb{R}^3$ of appropriate length (see Figure 2.3). More precisely, we have:

Theorem 2.2. *Assume (S) and let $p, q \in \partial\Omega$. Then, there exists a continuous and piecewise affine map $u : \bar{\Omega} \setminus L \to \mathbb{R}^3$ with the following properties:*

(i) u is an isometry, i.e.: $(\nabla u)^T \nabla u = Id_2$ almost everywhere in $\Omega \setminus L$,

(ii) the image $u(\sigma)$ of every geodesic σ from p to q in $\Omega \setminus L$, coincides with the segment $\overline{u(p)u(q)}$.

In particular, $|u(p) - u(q)| = length(\sigma)$ for each geodesic σ (as defined in (G)).

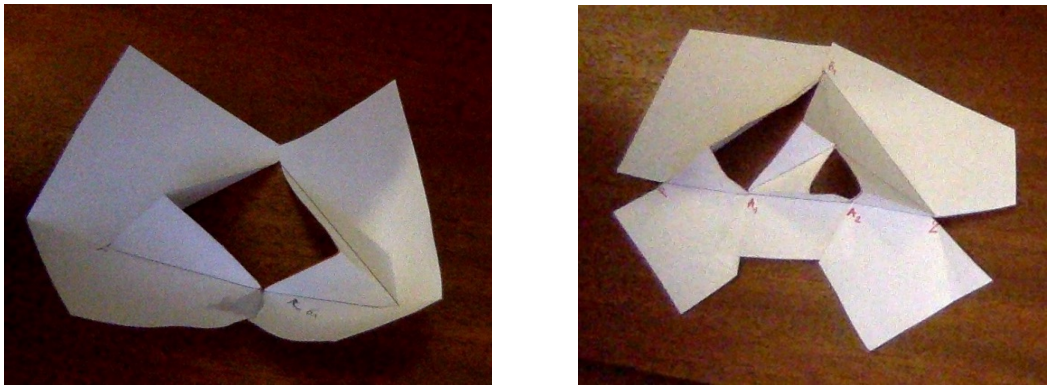

FIGURE 2.3. Examples of isometric immersions with properties as in Theorem 2.2, for configurations V, L, p, q as in Figure 2.1 (i) and (ii).

We prove Theorem 2.1 in section 3 and Theorem 2.2 in sections 4-8. Our proofs are constructive and describe: a specific algorithm to find the polygonal geodesics in Theorem 2.1, and a folding procedure that yields the isometric immersion u in Theorem 2.2. Even when all cuts in L are non-intersecting (i.e. the edges of the underlying graph G are pairwise disjoint), the construction of u is far from obvious. The general case requires a further refinement of the previous arguments, because of the completely arbitrary planar geometry of each connected component of G.

The algorithm that yields the isometry u in Theorem 2.2 consists of:

(i) identifying and sealing the portions of *inessential cuts*, which do not affect $\text{dist}(p, q)$;
(ii) ordering the geodesics and ordering the remaining cuts, that now form a new planar graph G consisting of *trees* (i.e. G is a forest);
(iii) constructing u on each region between two consecutive trees and two consecutive geodesics;
(iv) constructing u on regions within each tree;
(v) constructing u on the *exterior region* that is not enclosed by any two geodesics.

The points (i) and (ii) above are introduced in sections 4 and 5, respectively. The main arguments towards (iii) in the simplified setting are presented in section 6. The general case is resolved in section 7, which carries the heaviest technical load of this paper. Section 8 completes the proofs and presents an example explaining the necessity of p, q being located on the boundary of Ω in Theorem 2.2.

3. Proof of Theorem 2.1

Given $p, q \in \bar{\Omega} \setminus L$ and a piecewise $\mathcal{C}^1$ curve $\tau : [0, 1] \to \bar{\Omega} \setminus L$ with $\tau(0) = p$, $\tau(1) = q$, we first demonstrate a general procedure to produce a finite polygonal σ which joins p and q, whose other vertices are (not necessarily distinct) points in V, which satisfies condition (ii) in (G), and such that:

$$length(\sigma) \leq length(\tau).$$

Applying this procedure to curves τ with $length(\tau) \leq \mathrm{dist}(p,q)+1$ yields a family of polygonals with the listed properties, each of them having number of edges bounded by:

$$\frac{\mathrm{dist}(p,q)+1}{\min_{a_j \neq a_k} |a_j - a_k|}.$$

Hence, all geodesics from p to q in $\Omega \setminus L$ are precisely the length-minimizing polygonals among such (finitely many) polygonals. We further show that any length-minimizing polygonal satisfying condition (ii) of (G) cannot pass through the same vertex in V multiple times. Theorem 2.1 is then a direct consequence of these statements.

Without loss of generality, the path τ has no self-intersections. We construct σ by successive replacements of portions of τ by segments, as follows:

1. It is easy to show that for all $t > 0$ sufficiently small there holds: $\overline{p\tau(t)} \subset \bar{\Omega} \setminus L$. Set $\tau_1 = \tau$ and define:

$$t_1 = \sup\big\{t \in (0,1);\ \overline{p\tau_1(s)} \subset \bar{\Omega} \setminus L \ \text{ for all } \ s \in (0,t)\big\}, \quad q_1 = \tau_1(t_1).$$

There further holds: $t_1 \in (0,1]$ and $\overline{pq_1}$ is a geodesic from p to q_1. If $q_1 = q$ then we set $\sigma = \overline{pq}$ and stop the process. Otherwise, by construction, the segment $\overline{pq_1}$ must contain some of the vertices in V. Call p_1 the closest one of these points to q_1 and note that $p_1 \neq q_1$. Consider the concatenation of the segment $\overline{p_1 q_1}$ and the curve $\tau_{1|[t_1,1]}$. After re-parametrisation, it yields a piecewise $\mathcal{C}^1$ curve $\tau_2 : [0,1] \to \bar{\Omega}$, with the property that $\tau_2((0,1]) \subset \bar{\Omega} \setminus L$ and also:

$$|p - p_1| + length(\tau_2) \leq length(\tau).$$

2. We inductively define a finite sequence of endpoints $\{p_i\}_{i=2}^{k} \subset V$ and a sequence of piecewise $\mathcal{C}^1$ curves $\{\tau_i : [0,1] \to \bar{\Omega}\}_{i=3}^{k+1}$, by applying the procedure in Step 1 to curve τ_i and points $\tau_i(t_i) = p_i$ and q, until $q_{k+1} = q$ so that $\overline{p_k q}$ is a geodesic from p_k to q. Along the way, we get: $\tau_i(0) = p_i \neq p_{i-1}$, $\tau_i(1) = q$, $\tau_i((0,1]) \subset \bar{\Omega} \setminus L$, and:

$$\text{the sequence } \ \Big\{|p - p_1| + \sum_{j=2}^{j=i} |p_j - p_{j-1}| + length(\tau_{i+1})\Big\}_{i=1}^{k} \ \text{ is non-increasing.}$$

Also, the subset of $\bar{\Omega}$ enclosed by the concatenation of $\overline{pp_1 \dots p_i q_i}$ with the portion of the curve τ between p and q_i, contains no cuts in its interior. Consequently, each polygonal $\overline{pp_1 \dots p_i q_i}$ is a uniform limit of $\mathcal{C}^1$ curves contained in $\bar{\Omega} \setminus L$.

3. We finally define: $\sigma = \overline{pp_1 \dots p_k q}$.

The above process indeed terminates in a finite number k of steps, because the length of each polygonal $\overline{pp_1 \dots p_i}$ is bounded by $length(\tau)$, and at each step this length increases by at least: $\min_{a_j \neq a_k} |a_j - a_k| > 0$. See Figure 3.1 for an example of L, p, q, τ and the resulting polygonal σ.

The following observation concludes the proof of Theorem 2.1:

Lemma 3.1. *Let σ be a geodesic from p to q in $\Omega \setminus L$, as in (G). Then for every $a_i \in V$, there holds $a_i = \sigma(t)$ for at most one $t \in (0,1)$.*

Proof. We argue by contradiction and assume that a geodesic polygonal σ passes through some vertex $a_i \in V$ at least twice. Without loss of generality, we take a_i to be the first vertex in σ (counting

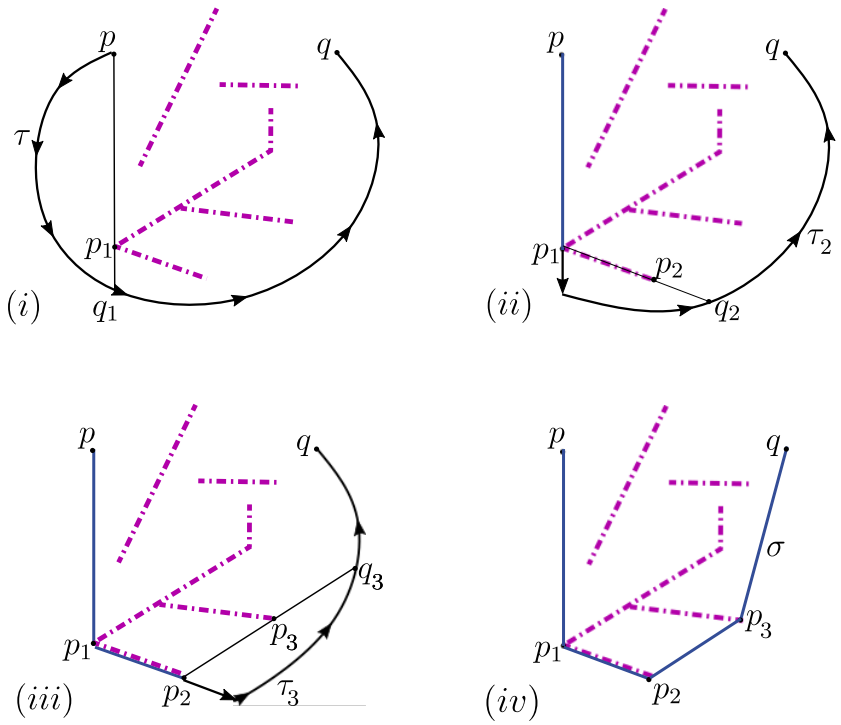

FIGURE 3.1. The path-shortening algorithm in the proof of Theorem 2.1.

from p) with this property. Consider the portion of σ containing the first and second occurrences of a_i, namely: $\overline{a_{i_0}a_ia_{i_1}a_{i_2}\dots a_{i_s}a_ia_{i_{s+1}}}$, and consider the approximating curve τ as in definition (G). From the approximate length-minimizing property of τ, it follows that both angles $\angle(a_{i_0}a_ia_{i_1})$ and $\angle(a_{i_s}a_ia_{i_{s+1}})$ must be at least π. Consequently, they are both equal to π. Another application of the same minimality condition yields that at least one of the segments $\overline{a_{i_0}a_i}$ and $\overline{a_ia_{i_{s+1}}}$ must be a cut in L. This contradicts with $p, q \notin L$ and a_i being the first multiple vertex of σ. ■

4. Proof of Theorem 2.2. Step 1: sealing the inessential cuts

Assume (S) and let p, q be two distinct points belonging to one connected component of $\bar{\Omega}\setminus L$. We describe a procedure which "seals" portions of cuts in L without decreasing the geodesic distance between p and q in $\Omega\setminus L$. First, consider $i = 1\dots n$ and $j,k = 1\dots\bar{n}$ so that $l_i = \overline{a_ja_k}$. Given $t \in \big[0, length(l_i)\big]$, define the altered endpoint of the cut l_i:

$$a_j(t) = (1-t)a_j + ta_k.$$

Let $L(t)$ be the new set of cuts in which l_i has been replaced by $l_i(t) = \overline{a_j(t)a_k}$, while all other cuts are left unchanged (this construction alters the V of the underlying graph G as well). We have the following observation:

Lemma 4.1. *With the above notation, the geodesic distance between p and q in $\Omega\setminus L(t)$:*

$$t \mapsto \mathrm{dist}_t(p,q) = \inf\big\{length(\tau);\ \tau:[0,1]\to\bar{\Omega}\setminus L(t)\ \textit{piecewise } \mathcal{C}^1,\ \textit{with } \tau(0)=p, \tau(1)=q\big\}$$

is left-continuous as a function of $t \in [0,1]$, and right-continuous in $t \in (0,1]$. It is also right-continuous at $t = 0$ when a_j is not the end-point of any other cut in L besides l_i.

Proof. Step 1. To prove the asserted left-continuity, take a sequence $\{t_m \in (0,1)\}_{m=1}^{\infty}$ that is strictly increasing to some $t_0 > 0$. It is clear that $\mathrm{dist}_{t_0}(p,q) \leq \liminf_{m\to\infty} \mathrm{dist}_{t_m}(p,q)$, because $\bar{\Omega} \setminus L(t_0) \subset \bar{\Omega} \setminus L(t_m)$ so that $\mathrm{dist}_{t_0}(p,q) \leq \mathrm{dist}_{t_m}(p,q)$ for all m.

For the reverse bound, fix $\epsilon > 0$ and let $\tau : [0,1] \to \bar{\Omega} \setminus L(t_0)$ be piecewise $\mathcal{C}^1$ with $\tau(0) = p$, $\tau(1) = q$, and such that $length(\tau) \leq \mathrm{dist}_{t_0}(p,q) + \epsilon$. We observe that if τ intersects $L(t_m)$, it must do so within $l_i(t_m) \setminus l_i(t_0)$. Since for sufficiently large m there holds: $length(l_i(t_m)) - length(l_i(t_0)) < \epsilon$, it follows that there exists $\tau_\epsilon : [0,1] \to \bar{\Omega} \setminus L(t_m)$ which is a local modification of τ, increasing its length by at most 2ϵ. Here, we are taking advantage of the fact that $a_j(t_m)$ is not the endpoint of any other cut besides $l_i(t_m)$ in $L(t_m)$. Consequently, we get:

$$\mathrm{dist}_{t_m}(p,q) \leq length(\tau_\epsilon) \leq \mathrm{dist}_{t_0}(p,q) + 3\epsilon.$$

Since $\epsilon > 0$ is arbitrary, this implies: $\limsup_{m\to\infty} \mathrm{dist}_{t_m}(p,q) \leq \mathrm{dist}_{t_0}(p,q)$.

Step 2. To show right-continuity of the function $\mathrm{dist}_t(p,q)$ at $t_0 \in (0,1)$, let $\{t_m \in (0,1)\}_{m=1}^{\infty}$ that is strictly decreasing to t_0. As in Step 1, we get: $\limsup_{m\to\infty} \mathrm{dist}_{t_m}(p,q) \leq \mathrm{dist}_{t_0}(p,q)$. In virtue of Theorem 2.1, for each m there holds:

$$\mathrm{dist}_{t_m}(p,q) = length\big(\overline{pa_{i_{1,m}}(t_m)a_{i_{2,m}}(t_m)\dots a_{i_{k(m),m}}(t_m)q}\big),$$

where for $s \neq i$ we set $a_s(t) = a_s$. Since the number of finite sequences of distinct indices chosen among $\{1\dots n\}$ equals $\sum_{k=1}^{n} k!$ and it is finite, it follows that at least one of such sequences $(i_1, i_2 \dots i_k)$ represents the order of the vertices in a geodesic polygonal as above, for infinitely many t_m-s. Passing to a subsequence if necessary, we may thus write:

$$\mathrm{dist}_{t_m}(p,q) = length\big(\overline{pa_{i_1}(t_m)a_{i_2}(t_m)\dots a_{i_k}(t_m)q}\big) \quad \text{for all } m.$$

We emphasize that at most one of the vertices changes as $m \to \infty$ and all others remain fixed. Further, as $m \to \infty$, the geodesics $\overline{pa_{i_1}(t_m)a_{i_2}(t_m)\dots a_{i_k}(t_m)q}$ converge to the polygonal $\sigma = \overline{pa_{i_1}\dots a_{i_k}q}$ that satisfies condition (ii) of (G). Consequently:

$$\lim_{m\to\infty} \mathrm{dist}_{t_m}(p,q) = length(\sigma) \geq \mathrm{dist}_{t_0}(p,q).$$

This concludes the proof of the lemma. The same argument is valid at $t_0 = 0$ under the indicated condition on a_j. ∎

We now define an inductive procedure in which lengths of all cuts are decreased as much as possible. Any resulting configuration $\bar{G}, \bar{V}, \bar{L}$ (see Figure 4.1 for examples) will be called *minimal*.

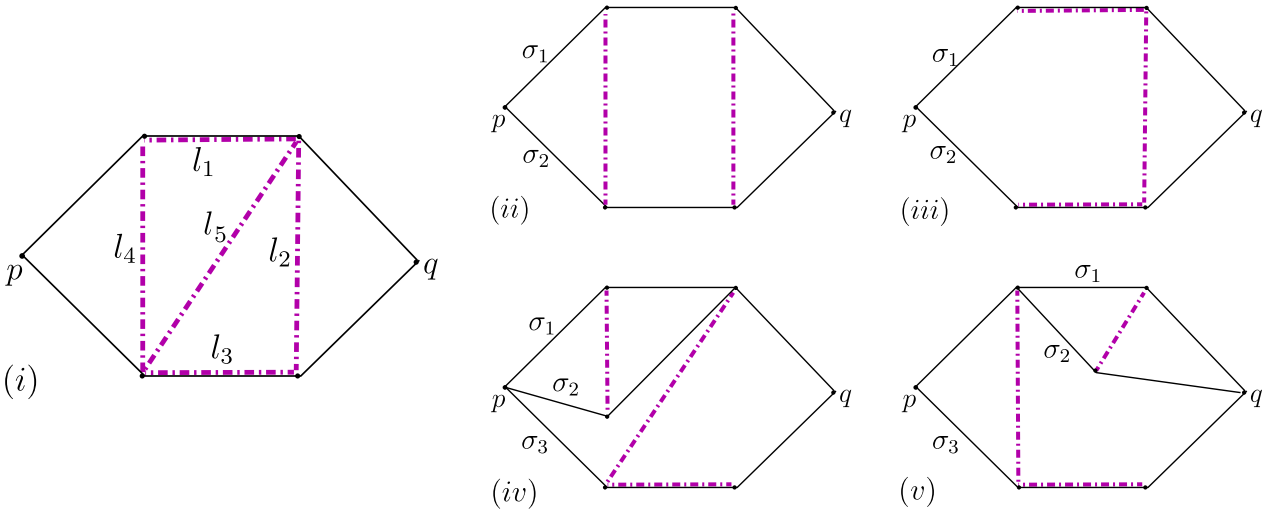

FIGURE 4.1. Different minimal configurations resulting from the original graph G in (i), obtained by the sealing procedure upon changing the order of edges in E and vertices in V: (ii) and (iii) yield two geodesics, while (iv) and (v) yield three geodesics.

1. Fix $i = 1$, write $l_1 = \overline{a_j a_k}$ and define:

$$t_1 = \sup\big\{t \in [0, length(l_1)];\ \mathrm{dist}_t(p,q) = \mathrm{dist}_0(p,q)\big\},$$

where $\mathrm{dist}_t(p,q)$ is as in Lemma 4.1. Replace the endpoint a_j by $a_j(t_1)$, and replace the cut l_1 by the segment $l_1(t_1) = \overline{a_j(t)a_k}$. If $a_j(t_1) = a_k$ then we remove l_1 altogether. Consider the problem of finding an isometric immersion u_1 with properties (i), (ii) in Theorem 2.2, for the same points p, q but with L replaced by $L_1 = L(t_1)$. Then $u = u_{1|\bar{\Omega}\setminus L}$ is a continuous, piecewise affine map fulfilling Theorem 2.2.

2. Write now $l_1 = \overline{a_k a_j}$ and let t_2 be defined as above, where we decrease the length of the already modified cut l_1 starting from the so far unaltered vertex a_k, up to $a_k(t_2)$. Replace l_1 by $l_2(t_2) = \overline{a_k(t_2)a_j}$ or remove it all together in case $a_k(t_2) = a_j$. Call the new set of cuts L_2.

3. Having constructed L_{2i} for some $1 \leq i < n$, consider the next cut $l_{i+1} = \overline{a_j a_k}$ and define:

$$t_{2i+1} = \sup\Big\{t \in \big[0, length(l_{i+1})\big];\ \mathrm{dist}_t(p,q) = \mathrm{dist}_0(p,q)\Big\},$$

where $\mathrm{dist}_t(p,q)$ is taken with respect to the previously obtained set of cuts L_{2i}. Replace the endpoint a_j by $a_j(t_{2i+1})$ and replace the cut $l_{i+1} \subset L_{2i}$ by $l_{i+1}(t_{2i+1})$. This defines the new collection of cuts $L_{2i+1} \subset L_{2i}$.

4. In the same manner, by possibly modifying the endpoint a_k of the already considered cut l_{i+1}, we construct the new set of cuts $L_{2i+2} \subset L_{2i+1}$.

5. We finally set:

$$\bar{L} = L_{2n}.$$

As in Step 1 of the algorithm, this ultimate collection $\bar{L} \subset L$ of cuts in Ω has the property that the validity of Theorem 2.2 for the configuration $p, q, \bar{L}$ implies its validity for the original configuration p, q, L.

Informally speaking, the above procedure starts by moving the first endpoint vertex of l_1 toward its second vertex, whereas we start "sealing" the portion of the cut l_1 left behind. The length of the geodesics connecting p and q may drop initially, in which case we leave the configuration unchanged. Otherwise, the geodesic distance is continuously nonincreasing, in view of Lemma 4.1 (it may initially remain constant). We stop the sealing process when the aforementioned distance becomes strictly less than the original one, and label the new position point as the new vertex endpoint of l_1. In the next step, we move the remaining endpoint along l_1 toward the (new) first endpoint and repeat the process, thus possibly sealing the cut l_1 further. The procedure is carried out for each l_i in the given order $i = 1, 2, \ldots, n$. We now claim that the distance between p and q cannot be further decreased, upon repeating the same process for the newly created configuration.

Lemma 4.2. *With respect to the cuts in $\bar{L} = \bigcup_{i=1}^{n} \bar{l}_i$, for any $i = 1 \ldots n$, any of the endpoint vertices of $\bar{l}_i$, and any $t > 0$ there holds:*

$$\mathrm{dist}_t(p, q) < \mathrm{dist}_0(p, q).$$

Proof. Denote $d = \mathrm{dist}_t(p, q)$ as above. At the $(2i-1)$-th step of construction of $\bar{L}$, we have:

$$d \leq \mathrm{dist}_{t_{2i-1}+t}(p, q),$$

because d corresponds to the geodesic distance between p and q in the complement of the cut set $\bar{L}$ with $\bar{l}_i$ further decreased, while $\mathrm{dist}_{t_{2i-1}+t}(p, q)$ corresponds to the geodesic distance in the subset of the aforementioned complement, obtained by enlarging all cuts $\{\bar{l}_j\}_{j>i}$ to their original lengths in L. On the other hand, directly by construction of $\bar{L}$ we get:

$$\mathrm{dist}_{t_{2i-1}+t}(p, q) < \mathrm{dist}_{t_{2i-1}}(p, q) = \mathrm{dist}_0(p, q).$$

This ends the proof of the lemma. ∎

Corollary 4.3. *The set of cuts $\bar{L}$ constructed above coincides with the set of edges $\bar{E}$ of the modified graph $\bar{G}$, with the new set of vertices $\bar{V}$, which have the following properties:*

(i) $\bar{G}$ has no loops, and consequently it is a forest, consisting of finitely many trees,
(ii) each vertex in $\bar{V}$ that is an endpoint of only one edge in $\bar{E}$ (i.e. a leaf of the forest $\bar{G}$), is a vertex of some geodesic σ from p to q in $\Omega \setminus \bar{L}$.

Proof. Step 1. To prove (i), we show that $\mathbb{R}^2 \setminus \bar{L}$ must be connected. Indeed, in the opposite case, the boundary of the connected component R_1 of $\mathbb{R}^2 \setminus \bar{L}$ containing p and q, must contain a cut $\overline{a_j a_k}$ that is also a part of the boundary of some other connected component R_2 of $\mathbb{R}^2 \setminus \bar{L}$. By the minimality property of $\bar{L}$ in Lemma 4.2, it follows that the sealing procedure with respect to the indicated cut $\overline{a_j a_k}$ and its endpoint a_j results in the decrease of $\mathrm{dist}_t(p, q)$ for any $t > 0$. Consequently, there exists a piecewise $\mathcal{C}^1$ curve $\tau : [0, 1] \to \bar{\Omega} \setminus \bar{L}(t)$ with $\tau(0) = p$, $\tau(1) = q$ and $length(\tau) < \mathrm{dist}_0(p, q)$, where this last distance is taken in $\Omega \setminus \bar{L}$. The curve τ must both enter and exit R_2 through the segment $\overline{a_j a_j(t)}$. This means that τ may be further shortened by replacing its portion contained in the aforementioned interior region by an appropriate straight segment. The resulting curve is $\bar{\tau} : [0, 1] \to \Omega \setminus \bar{L}$, with:

$$length(\bar{\tau}) < length(\tau) < \mathrm{dist}_0(p, q),$$

which is a contradiction.

Step 2. Let $a_i \in \bar{V}$ be as requested in (ii). Consider the modified endpoints $a_i(1/m)$ and the cut collections $\bar{L}(1/m)$ as described in the sealing algorithm. As in the proof of Lemma 4.1, there must

exist a finite sequence $(i_1, \dots, i_k)$ such that:

$$\sigma_m = \overline{a_{i_1}(1/m)a_{i_2}(1/m)\dots a_{i_k}(1/m)}$$

is a geodesic from p to q in $\Omega \setminus \bar{L}(1/m)$ for infinitely many m-s. By the maximality assertion in Lemma 4.2, there must be: $i \in \{i_1, \dots, i_k\}$. But then Lemma 4.1 yields:

$$\mathrm{dist}_0(p,q) = \lim_{m\to\infty} \mathrm{dist}_{1/m}(p,q) = \lim_{m\to\infty} length(\sigma_m) = length(\overline{pa_{i_1}\dots a_{i_k}q}).$$

Consequently, $\overline{pa_{i_1}\dots a_{i_k}q}$ is a geodesic from p to q in $\Omega \setminus \bar{L}$, whose existence is claimed in (ii). ■

Remark 4.4. When the minimal configuration $\bar{L}$ consists of disjoint segments $\{l_i\}_{i=1}^n$, then each geodesic σ from p to q in $\Omega \setminus \bar{L}$ does not contain any cuts. Indeed, assume by contradiction that $\bar{l} \subset \sigma$, for some cut $\bar{l} \subset \bar{L}$. Denote $\bar{\bar{L}} = \bar{L} \setminus \bar{l}$, then by the maximality condition in Lemma 4.2, there exists a piecewise $\mathcal{C}^1$ curve τ from p to q in $\Omega \setminus \bar{\bar{L}}$ satisfying $length(\tau) < length(\sigma)$. Hence, τ must intersect $\bar{l}$ at only one point which we call x. Consider two piecewise $\mathcal{C}^1$ curves: the curve τ_1 obtained by concatenating the portion of τ from p to x, with the portion of σ from x to q, and the curve τ_2 obtained by concatenating the portion of σ from p to x, with the portion of τ from x to q. One of these curves, say τ_1, must satisfy:

$$length(\tau_1) < length(\sigma).$$

But then one can approximate τ_1 by another piecewise $\mathcal{C}^1$ curve $\bar{\tau}_1 : [0,1] \to \Omega \setminus \bar{L}$ (see Figure 4.2 (i)), to the effect that $length(\bar{\tau}_1) < length(\sigma)$, which contradicts σ being a geodesic. Note that in the general case of $\bar{L}$ supported on the minimal graph $\bar{G}$ with vertex degrees possibly exceeding 1, the above property is no more true (see Figure 4.2 (ii)).

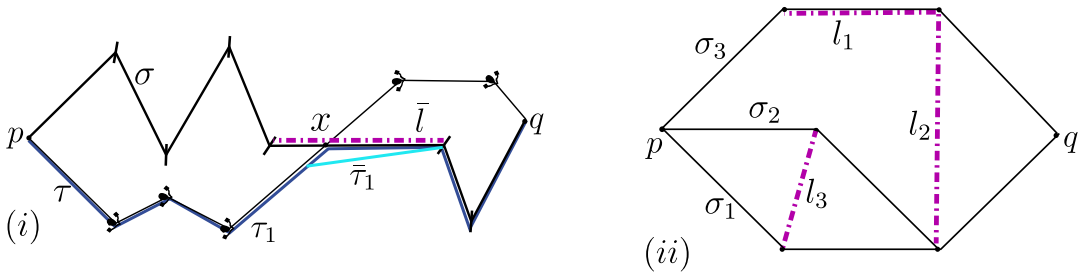

FIGURE 4.2. Concatenating and shortening of the geodesic in Remark 4.4. In (i), the turning vertices of the base polygonals σ and τ are indicated by, respectively, dashes and mid-markers. The concatenated shortened polygonal τ_1 is in blue; it can be approximated by a polygonal $\bar{\tau}_1$ with values in $\Omega \setminus \bar{L}$, by means of a segment (in light blue) that avoids $\bar{l}$. In (ii) the displayed configuration of cuts is minimal, yet cuts are not separated. There are three geodesic polygonals $\{\sigma_i\}_{i=1}^3$ from p to q.

5. Proof of Theorem 2.2. Step 2: ordering the geodesics

Assume (S) and let p, q be two distinct points belonging to one connected component of $\bar{\Omega} \setminus L$. In the previous section we showed that, without loss of generality, the set of cuts $L = \bigcup_{i=1}^n l_i$ satisfies assertions in Corollary 4.3. From now on, we work assuming these additional properties and denote by (G, V, L) a minimal configuration (instead of the notation $(\bar{F}, \bar{V}, \bar{L})$ used in section 4).

The (finite, nonempty) set of all geodesics from p to q in $\Omega \setminus L$ has a partial order relation $\preceq$ in:

(O) Given two geodesics from p to q in $\Omega \setminus L$:

$$\sigma_1 = \overline{pa_{i_1}a_{i_2}\dots a_{i_k}q}, \qquad \sigma_2 = \overline{pa_{j_1}a_{j_2}\dots a_{j_s}q},$$

we write $\sigma_1 \preceq \sigma_2$ provided that the concatenated polygonal:

$$\sigma = \sigma_1 * (\sigma_2)^{-1} = \overline{pa_{i_1}a_{i_2}\dots a_{i_k}qa_{j_s}a_{j_{s-1}}\dots a_{j_1}p}$$

is the boundary of (finitely many) open bounded connected regions in $\mathbb{R}^2$, and moreover σ is oriented counterclockwise with respect to all of these regions.

Lemma 5.1. *In the above setting, we have:*

(i) there exist the unique geodesic σ_{min} and the unique geodesic σ_{max} such that $\sigma_{min} \preceq \sigma \preceq \sigma_{max}$ for all geodesics σ from p to q in $\Omega \setminus L$; we call σ_{min} the least and σ_{max} the greatest geodesic,

(ii) there exists a chain of geodesics $\sigma_1 \preceq \sigma_2 \dots \preceq \sigma_N$, such that $\sigma_1 = \sigma_{min}$, $\sigma_N = \sigma_{max}$ and that the consecutive geodesics cover each other, i.e. for all $i = 1 \dots N-1$ there holds: $\sigma_i \neq \sigma_{i+1}$ and if $\sigma_i \preceq \sigma \preceq \sigma_{i+1}$ for some other geodesic σ, then $\sigma = \sigma_i$ or $\sigma = \sigma_{i+1}$.

Proof. Step 1. For the least geodesic statement in (i), it suffices to show that if σ_1, σ_2 are two minimal elements for the partial order $\preceq$, then necessarily $\sigma_1 = \sigma_2$. To this end, we will construct a geodesic σ with $\sigma \preceq \sigma_1$ and $\sigma \preceq \sigma_2$. The statement for the greatest geodesic follows by a symmetric argument.

We write: $\sigma_1 = \overline{pa_{i_1}a_{i_2}\dots a_{i_k}q}$ and $\sigma_2 = \overline{pa_{j_1}a_{j_2}\dots a_{j_s}q}$. Observe first that σ_1 and σ_2 cannot have a common point $x \notin \{p, q\}$ that is not a vertex in V, unless they have a common edge $\overline{a_{i_m}a_{i_{m+1}}} = \overline{a_{j_l}a_{j_{l+1}}}$, then containing x. Indeed, in the aforementioned situation, both polygonals: τ_1 obtained by concatenating the portion of σ_1 from p to x, with the portion of σ_2 from x to q, and τ_2 concatenating the portion of σ_2 from p to x, with the portion of σ_1 from x to q, would satisfy:

$$length(\tau_1) = length(\tau_2) = length(\sigma_1) = length(\sigma_2).$$

Similarly to the construction in the proof of Corollary 4.3, see also Figure 4.2, we could then approximate τ_1 (and also τ_2) by a piecewise $\mathcal{C}^1$ curve $\tau : [0,1] \to \bar{\Omega} \setminus L$ with $length(\tau)$ strictly less than the four coinciding lengths above. This would contradict σ_i-s being geodesics.

Let $a_{i_m} = a_{j_l}$ be the first common vertex of σ_1 and σ_2, beyond p. If $i_m = i_1$ and $j_l = j_1$, then we include $\overline{pa_{i_1}}$ as the starting portion of σ; otherwise we choose $\overline{pa_{i_1}a_{i_2}\dots a_{i_m}}$ in case the concatenation $\overline{pa_{i_1}\dots a_{i_m}a_{j_{l-1}}\dots a_{j_1}p}$ has the counterclockwise orientation with respect to the bounded open region it encloses, or $\overline{pa_{j_1}a_{j_2}\dots a_{j_l}}$ in the reverse case. Let $a_{i_{\bar{m}}} = a_{j_{\bar{l}}}$ be the second common vertex of σ_1 and σ_2, beyond a_{i_m}; we choose the least of $\overline{a_{i_m}\dots a_{i_{\bar{m}}}}$ and $\overline{a_{j_l}\dots a_{j_{\bar{l}}}}$, as above, to be concatenated with the previous portion of σ. By such inductive procedure, we obtain a required geodesic σ that satisfies $\sigma \preceq \sigma_1$ and $\sigma \preceq \sigma_2$. From minimality, it follows that $\sigma = \sigma_1 = \sigma_2$, and so $\sigma = \sigma_{min}$ is the least element for $\preceq$.

Step 2. To prove (ii), we set $\sigma_1 = \sigma_{min}$ and $\sigma_N = \sigma_{max}$ for some $N \geq 2$. If σ_N covers σ_1, then $\sigma_1 \preceq \sigma_N$ is the required chain. Otherwise, there exists a geodesic $\sigma \notin \{\sigma_1, \sigma_N\}$ such that $\sigma_1 \preceq \sigma \preceq \sigma_N$. If σ covers σ_1 then we write $\sigma_2 = \sigma$, if it is covered by σ_N then we set $\sigma_{N-1} = \sigma$. If none of the above holds, there must exist a geodesic $\tau \notin \{\sigma_1, \sigma, \sigma_N\}$ such that:

$$\sigma_1 \preceq \tau \preceq \sigma \quad \text{or} \quad \sigma \preceq \tau \preceq \sigma_N.$$

We continue in this fashion until the process is stopped, which will occur in finitely many steps due to the finite number of geodesics from p to q in $\Omega \setminus L$. ∎

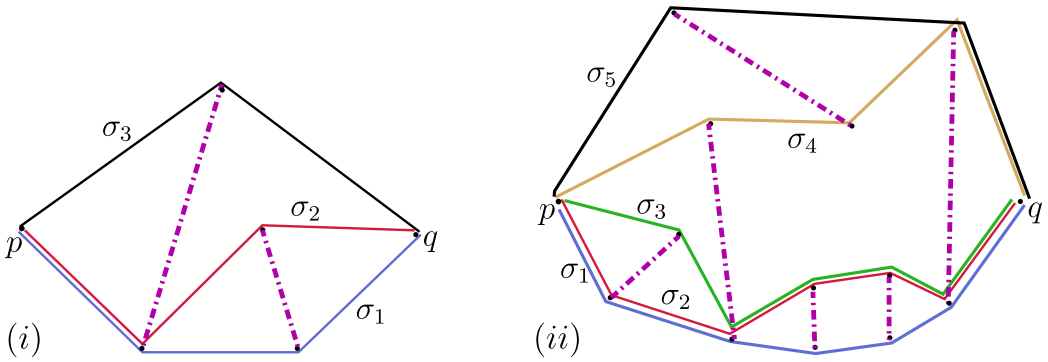

FIGURE 5.1. Examples of sequence of geodesics produced in Lemma 5.1: diagram (i) refers to the configuration L, p, q in Figure 2.1 (ii) where the resulting sequence consists of the following geodesics: $\sigma_1 = \sigma_{min}$ in blue, σ_2 in red and $\sigma_3 = \sigma_{max}$ in black; in a more complex diagram (ii) the sequence consists of: $\sigma_1 = \sigma_{min}$ in blue, σ_2 in red, σ_3 in green, σ_4 in brown and $\sigma_5 = \sigma_{max}$ in black.

Lemma 5.2. *In the above setting, let $\sigma_1 \preceq \sigma_2 \ldots \preceq \sigma_N$ be as in Lemma 5.1 (ii). For each $r = 1 \ldots N-1$, let R_r be the open, bounded region enclosed by the concatenation $\sigma_r * (\sigma_{r+1})^{-1}$. We set $R_0 = \Omega \setminus \bigcup_{r=1}^{N-1} \bar{R}_r$ to be the exterior region relative to the concatenation $\sigma_1 * (\sigma_N)^{-1}$. Then, for each tree T that is a connected component of G, there holds:*

(i) T has nonempty intersection with the interior of exactly one region $\bar{R}_r$,
(ii) if $T \subset \bar{R}_r$ for $r = 1 \ldots N-1$, then T has vertices on both σ_r and σ_{r+1}.

Moreover, if $p, q \in \partial\Omega$, then there are no trees in R_0.

Proof. Step 1. If T violated the condition in (i) then there would exist a path $\alpha \subset T$ and two distinct points $A, B \in \alpha$ (which are not necessarily the vertices in V) such that $A \in R_{r-1}$, $B \in R_r$ for some $r = 1 \ldots N$ (where we set $R_N = R_0$), and such that the portion of α between A and B crosses the geodesic σ_r. This would contradict condition (ii) in definition (G).

Step 2. To prove (ii), assume without loss of generality that all vertices of a maximal tree $T \subset \bar{R}_r$ belong to σ_r. Call A the leaf of T that is closest to p along σ_r, and B the leaf that is closest to q. By Corollary 4.3 (ii) and since each tree has at least two leaves, there must be $A \neq B$. Consider the (unique) path $\alpha \subset T$ connecting A and B. If $\alpha \subset \sigma_r$, then there would be $T = \alpha$. Also, in this case α together with edges of σ_r immediately preceding A and immediately succeeding B would form a straight segment, contradicting the minimality of G. Thus, α passes through R_r.

Call A' the first vertex on α whose immediate successor belongs to R_r, and B' the last vertex whose immediate predecessor belongs to R_r; there may be $A' = A$ or $B' = B$. Call $\alpha' = \overline{A' a_{i_1} \ldots a_{i_l} B'} \subset \alpha$ the unique path in T connecting A' with B', and denote by $D \subset R_r$ the region enclosed by the concatenation of α' and the portion of σ_r between A' and B'.

We now label each vertex $a_{i_s} \in \alpha' \setminus \sigma_r$ as *type I/II from left*, provided that there exists a sequence of piecewise $\mathcal{C}^1$ paths $\{\tau_k : [0,1] \to \bar{\Omega} \setminus L(1/k)\}_{k=1}^{\infty}$ with $\tau_k(0) = p$, $\tau_k(1) = q$ and $length(\tau_k) < \text{dist}(p,q)$, where $L(1/k)$ denotes the modified cut set L in which the edge $\overline{a_{i_{s-1}} a_{i_s}}$ in the graph G is replaced by the shortened segment $\overline{a_{i_{s-1}} a_{i_s}(1/k)}$ with $a_{i_s}(1/k) = a_{i_s} - \frac{1}{k}(a_{i_s} - a_{i_{s-1}})$. Further, we request that:

Type I from left: each τ_k *enters* D, only once, through the removed segment portion $\overline{a_{i_s}(1/k) a_{i_s}}$.
Type II from left: each τ_k *exits* the region D, only once, through $\overline{a_{i_s}(1/k) a_{i_s}}$.

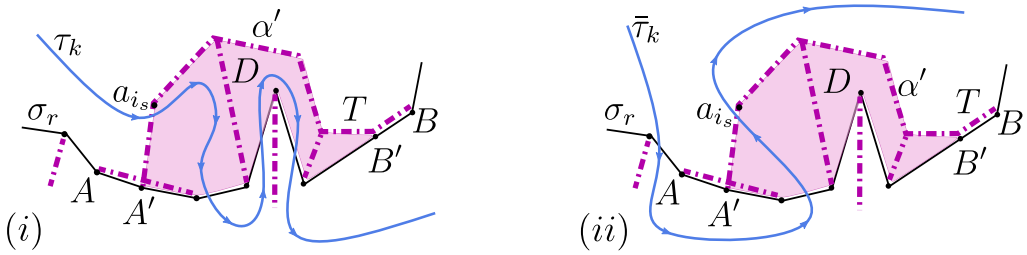

FIGURE 5.2. Notation in the proof of Lemma 5.2, Step 2: in (i) the curve τ_k enters the (shaded) region D, hence the indicated vertex $a_{i_s} \in \alpha'$ is of type I from left; in (ii), existence of a shortening path $\bar\tau_k$ which exits D via the removed edge portion preceding a_{i_s} in α', implies that a_{i_s} is of type II from left.

Similarly, we label $a_{i_s} \in \alpha' \setminus \sigma_r$ as *type I/II from right*, when there exists a sequence of piecewise $\mathcal{C}^1$ paths $\{\bar\tau_k : [0,1] \to \bar\Omega \setminus \bar L(1/k)\}_{k=1}^{\infty}$ with $\bar\tau_k(0) = p$, $\bar\tau_k(1) = q$, $length(\bar\tau_k) < \mathrm{dist}(p,q)$, and where $\bar L(1/k)$ stands for the modified cut set L in which $\overline{a_{i_s}a_{i_{s+1}}}$ is replaced by $\overline{a_{i_s}(1/k)a_{i_{s+1}}}$ with $a_{i_s}(1/k) = a_{i_s} + \frac{1}{k}(a_{i_{s+1}} - a_{i_s})$. Moreover, we request that:

Type I from right: each $\bar\tau_k$ *enters* D, only once, through the removed segment portion $\overline{a_{i_s}a_{i_s}(1/k)}$.
Type II from right: each $\bar\tau_k$ *exits* D, only once, through $\overline{a_{i_s}a_{i_s}(1/k)}$.

In the definitions above (see diagrams in Figure 5.2), we set $a_{i_0} = A'$ and $a_{i_{l+1}} = B'$. By the minimality of G, each a_{i_s} must be of type I or type II from left (it may be both), and it must be of type I or type II from right (it may be both).

Step 3. We claim that a_{i_1} has to be of type I from left. We argue by contradiction and hence assume that a_{i_1} is of type II from left. Note that the length of the portion of the shortening curve $\bar\tau_k$ between p and the exit point from D is strictly larger than the distance from p to a_{i_1} in $\Omega \setminus L$, because all the internal (with respect to R_r) angles along α from A to A' are not greater than π, whereas the angle at A' is strictly smaller than π. Concatenating with the remaining portion of $\bar\tau_k$ and taking the limit $k \to \infty$, it follows that there is a geodesic from p to q in $\Omega \setminus L$ passing through a_{i_1}. This contradicts the fact that $a_{i_1} \notin \sigma_k$, and proves the claim.

By a similar argument, we can show that if a_{i_s} is of type I from left, then it is also of type I from right. We argue by contradiction and hence assume that a_{i_s} is of type II from right. Consider the curves τ_k and $\bar\tau_k$ corresponding to the two assumed properties of a_{i_s}; they must intersect at some point C occurring after τ_k enters D and before $\bar\tau_k$ exits from D. Define the curves: η_k as the concatenation of the portion of τ_k from p to C with the portion of $\bar\tau_k$ from C to q, and $\bar\eta_k$ as the concatenation of the portion of $\bar\tau_k$ from p to C with the portion of τ_k from C to q. Since $\bar\eta_k \subset \Omega \setminus L$, it follows that $length(\bar\eta_k) \geq \mathrm{dist}(p,q)$. Consequently:

$$length(\eta_k) = length(\tau_k) + length(\bar\tau_k) - length(\bar\eta_k) < \mathrm{dist}(p,q).$$

The only possibility for this when taking the limit $k \to \infty$, we obtain the existence of a geodesic from p to q in $\Omega \setminus L$ passing through a_{i_s}. This contradicts the fact that a_{i_s} is not on any geodesic.

Finally, we argue that if a_{i_s} is of type I from right, then the next vertex $a_{i'_s}$ on α' that belongs to R_r must be of type I from left as well. If not, then $a_{i'_s}$ is of type II from left and we can define the point C and the concatenated curves η_k and $\bar\eta_k$ as in the previous reasoning. Again, $length(\bar\eta_k) \geq \mathrm{dist}(p,q)$, so $length(\eta_k) < \mathrm{dist}(p,q)$. However, we may replace the portion of η_k between the entry point of

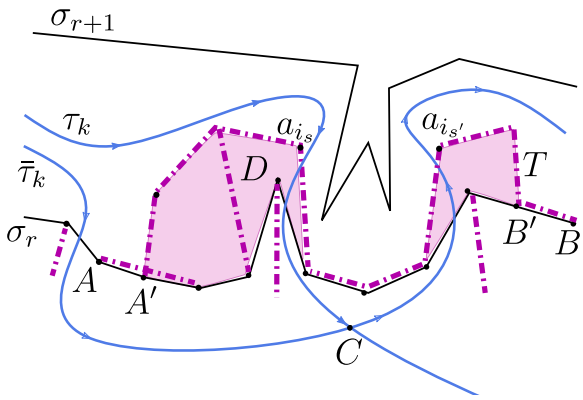

FIGURE 5.3. Concatenating curves τ_k and $\bar\tau_k$ at the intersection C in the proof of Lemma 5.2 Step 3, when the region D has multiple connected components.

τ_k to D, and the exit point of $\bar\tau_k$ from D, by a shorter curve (see Figure 5.3) which is completely contained in $\Omega\setminus L$. Indeed, when $i_{s'}=i_{s+1}$, then the said curve may follow the segment $\overline{a_{i_s}a_{i_{s'}}}\subset\alpha'$. When $i_{s'}\neq i_{s+1}$, then the portion of the polygonal α' between a_{i_s} and $a_{i_{s'}}$ has all internal angles (with respect to R_r) not greater than π, so one can simply take the geodesic from a_{i_s} to $a_{i_{s'}}$ in $\Omega\setminus L$. As a consequence and passing to the limit with $k\to\infty$, we obtain a geodesic from p to q in $\Omega\setminus L$ passing through a_{i_s} and $a_{i_{s'}}$. This contradicts $a_{i_s},a_{i_{s'}}$ not being on any geodesic.

Step 4. Applying the observations from Step 3, it follows that the vertex a_{i_l} must be of type I from right. However this is impossible by a symmetric argument to a_{i_1} not being of type II from left. This ends the proof of (ii). In case $p,q\in\partial\Omega$, the region R_0 consists of two connected components, and hence any tree $T\in R_0$ would have vertices either only on σ_1 or only on σ_N. By the same arguments as above, this is impossible, which implies the final statement of the lemma. ∎

We close the above discussion by pointing out that in case $p,q\notin\partial\Omega$, there may be a tree (or even multiple trees) in R_0, with vertices both on σ_1 and σ_N (see Figure 8.1 in section 8). The next main result of this section allows for the lexicographic ordering of the connected components of $\bar\Omega\setminus L$. Namely, we have (see example in Figures 5.4 and 5.5):

Lemma 5.3. *In the above setting, let $\sigma_1\preceq\sigma_2\ldots\preceq\sigma_N$ be as in Lemma 5.1 (ii). Fix $r=1\ldots N-1$ and consider the region R_r enclosed between two consecutive geodesics $\sigma_r=\overline{pa_{i_1}a_{i_2}\ldots a_{i_k}q}$ and $\sigma_{r+1}=\overline{pa_{j_1}a_{j_2}\ldots a_{j_l}q}$, as in Lemma 5.2. Consider further the set of maximal trees $\{T_m\}_{m=1}^s$ which are the connected components of G contained in $\bar R_r$. Then we have:*

(i) the ordering $T_1,\ldots,T_s$ can be made so that each leaf of T_i on σ_r (respectively σ_{r+1}) precedes each leaf of T_j on σ_r (resp. σ_{r+1}), when $i<j$.

The region $R_r\setminus L$ is the union of $s+1$ (open) polygons $\{P_m\}_{m=0}^s$ and of additional families of polygons $\{Q_m\}_{m=1}^s$, described as follows:

(ii) we denote $\alpha_0^{left}=\overline{p_1p_1}$ and $\alpha_s^{right}=\overline{q_1q_1}$, where p_1,q_1 are two common vertices of σ_r and σ_{r+1}, such that $\overline{pa_{i_1}\ldots p_1}=\overline{pa_{j_1}\ldots p_1}$ and $\overline{q_1\ldots a_{i_k}q}=\overline{q_1\ldots a_{j_l}q}$ (we take the last, along σ_r, vertex with the said property to be p_1 and the first vertex to be q_1). For each $m=1\ldots s$ we denote α_{m-1}^{right} (respectively, α_m^{left}) the unique path in T_m joining its first (resp. its last) vertex on σ_r with its first (resp. the last) vertex on σ_{r+1}, both counting from p_1. Note that there may be $\alpha_m^{left}=\alpha_{m-1}^{right}$. Then, the boundary of each P_m consists of paths α_m^{left}, α_m^{right} and of

the intermediate portions of σ_r and σ_{r+1} which are concave with respect to P_m. Namely, all interior angles of P_m which are not on $\alpha_m^{left} \cup \alpha_m^{right}$ are not less than π. Finally, there are no cuts in P_m.

(iii) each family Q_m consists of finitely many polygons Q_m^f, that are the connected components of $R_r \setminus L$ enclosed between α_m^{left}, α_{m-1}^{right} and the portions of σ_r and σ_{r+1}. The boundary of each Q_m^f consists of a single path within T_m plus a single portion of the geodesic σ_r or σ_{r+1}. It has all interior angles not at vertices belonging of T_m concave with respect to R_m.

Proof. For (i), consider first σ_r and recall that each vertex $a_{i_1}, \dots, a_{i_k}$ is an endpoint of some cut, which belongs to some maximal tree $T \subset G$. If T extends inside the region R_r, then it must have vertices on both σ_r and σ_{r+1}, by Lemma 5.2. The same reasoning can be applied to cuts emanating from σ_{r+1}. We can now order the trees $\{T_m\}_{m=1}^s$, based on how many vertices (along σ_r and σ_{r+1}) separate their leaves from p. This ordering is well defined, as trees are non-intersecting. Assertions (ii) and (iii) follow directly by construction and since σ_r, σ_{r+1} are geodesics. ∎

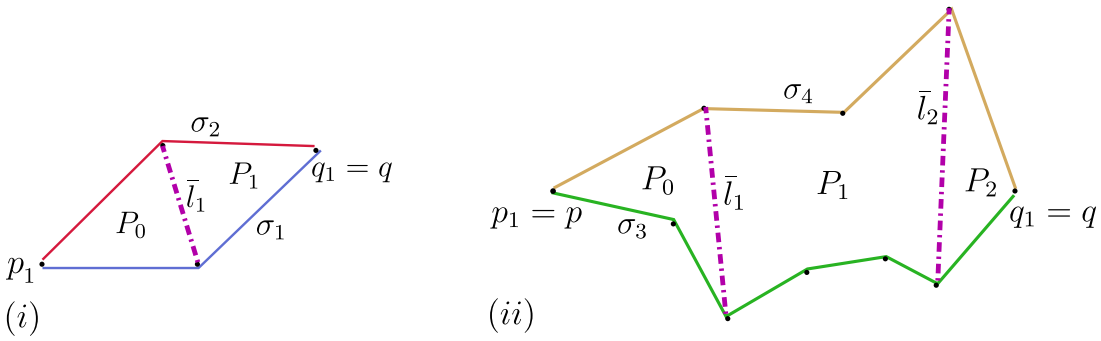

FIGURE 5.4. Partitions $\{P_m\}_{m=0}^s$ defined in Lemma 5.3: (i) depicts partition of the region R_1 corresponding to Figure 5.1 (i), while (ii) depicts the region R_3 in Figure 5.1 (ii). In both figures the trees T_m coincide with paths $\alpha_{m-1}^{right} = \alpha_m^{left}$ that are single cuts, and consequently all intermediate polygonal collections Q_m are empty.

Concluding, we see that the assumption (S) may be replaced by the following modified setup:

(S1)
The set of cuts L satisfies assertions of Corollary 4.3. The chain of geodesics $\{\sigma_r\}_{r=1}^N$, each from p to q in $\Omega \setminus L$, satisfies condition in Lemma 5.1 (ii) with respect to the partial order in (O). In agreement with Lemma 5.3, the set $\Omega \setminus L$ is partitioned into N regions $\{R_r\}_{r=0}^N$:
- (i) for each $r = 1 \dots N-1$, the "interior" bounded region R_r which is enclosed by $\sigma_r * (\sigma_{r+1})^{-1}$, and partitioned into polygonal sub-regions $\{P_m\}_{m=0}^s \cup \{Q_m\}_{m=1}^s$ corresponding to the consecutive trees $\{T_m\}_{m=1}^s$ (we suppress the dependence on r in this notation), as specified in Lemma 5.3,
- (ii) the "exterior" region $R_0 = \Omega \setminus \bigcup_{r=1}^{N-1} \bar{R}_r$.

We also define the segment $I = \overline{0, length(\sigma_1)e_1} \subset \mathbb{R}^3$.

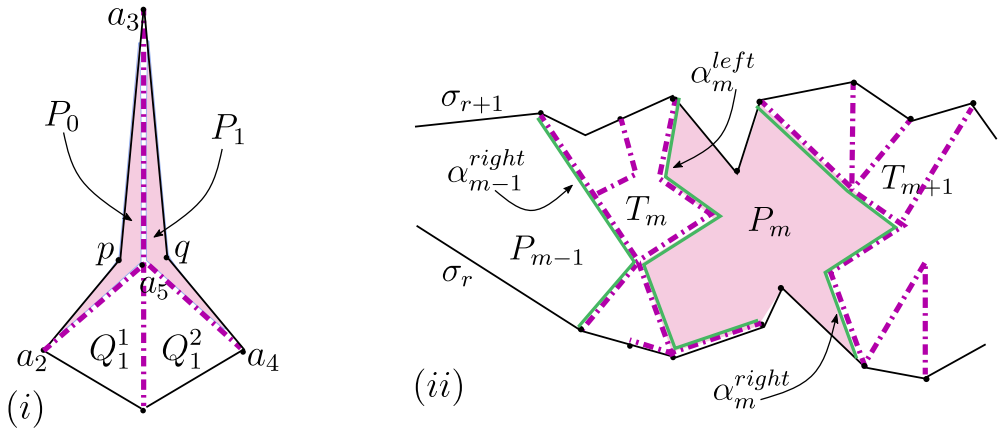

FIGURE 5.5. Polygons $\{P_m\}_{m=0}^s$ and polygon families $\{Q_m\}_{m=1}^s$ defined in Lemma 5.3: (i) corresponds to the unique region R_1 in Figure 2.2 (iii) with paths: $\alpha_0^{left} = \overline{pp}$, $\alpha_0^{right} = \overline{a_2a_5a_3}$, $\alpha_1^{left} = \overline{a_4a_5a_3}$, $\alpha_1^{right} = \overline{qq}$; (ii) is a general diagram depicting the partition of the region R_r.

6. Proof of Theorem 2.2, a simplified case. Step 3: isometric immersion on interior regions between consecutive cuts

Assume (S) and let p, q be two distinct points in $\bar{\Omega} \setminus L$. In view of the results in previous sections, the goal is to construct an isometry u as in Theorem 2.2, separately on each R_r identified in (S1). We first concentrate on the interior case $r = 1 \dots N-1$, while in section 8 we address the case $r = 0$.

In this section we treat a simplified scenario in which all trees $T_1, \dots, T_s$ consist of single cuts; note that this occurs, in particular, if all cuts in the original graph G are non-intersecting:

Lemma 6.1. *Assume (S) and (S1). Fix $r = 1 \dots N-1$ and further assume that:*

$$T_m = \bar{l}_m = \overline{a_{m_1} a_{m_2}} \quad \text{for all } \ m = 1 \dots s.$$

Then there exists a continuous, piecewise affine isometric immersion $u : R_r \setminus \bigcup_{m-1}^s \bar{l}_m \to \mathbb{R}^3$, with:

$$u(p) = 0, \quad u(q) = length(\sigma_1)e_1, \quad u(\sigma_r) = u(\sigma_{r+1}) = I.$$

Proof. We will inductively find the matching isometric immersions u of the consecutive polygons $\{P_m\}_{m=0}^s$. Note that polygons in $\bigcup_{m=1}^s Q_m$ are absent in the presently discussed case.

Step 1. On P_0, we first fold its "top" part so that the image of the portion of σ_{r+1} from p_1 to the endpoint B_1 of the cut $\bar{l}_1 = \overline{A_1B_1}$ coincides with the sub-interval:

$$\overline{length(\overline{pa_{i_1} \dots p_1})e_1, length(\overline{pa_{i_1} \dots B_1})e_1} \subset I.$$

This can be achieved because all internal angles of σ_{r+1} at vertices between (but not including) p_1 and B_1 are at least π. A symmetric fold construction can be performed on the "bottom" part of P_0, along the boundary portion contained in σ_r.

As a result, the vector $u(B_1) - u(A_1)$ equals $\big(length(\overline{pa_{i_1} \dots B_1}) - length(\overline{pa_{j_1} \dots A_1})\big)e_1$ and we consecutively have to find an isometric immersion of the polygon P_1 with the property that writing $\bar{l}_2 = \overline{A_2B_2}$ with $A_2 \in \sigma_r, B_2 \in \sigma_{r+1}$, the length of the vector $\big(u(B_2) - u(A_2)\big) - \big(u(B_1) - u(A_1)\big)$ is prescribed, and that the images of portions of: geodesic σ_r between A_1 and A_2, and of geodesic σ_{r+1} between B_1 and B_2, are contained in $\mathbb{R}e_1$.

Step 2. Assume that u has been constructed on $P_1 \cup \dots P_{m-1}$, for some $m \leq s-1$. Consider the polygon P_m and the two related closed convex sets S_A and S_B. The set S_B is defined by specifying its boundary to consist of: the portion of σ_{r+1} between the endpoints B_m and B_{m+1} of the cuts $\bar{l}_m$, $\bar{l}_{m+1}$, respectively, and of the segment $\overline{B_m B_{m+1}}$. The boundary of the set S_A is: the portion of σ_r between the remaining endpoints A_m and A_{m+1} of the cuts $\bar{l}_m$, $\bar{l}_{m+1}$, and of the segment $\overline{A_m A_{m+1}}$. We note that the interior of the defined sets may be empty; for example if $\overline{A_m A_{m+1}} \subset \sigma_r$ then $S_A = \overline{A_m A_{m+1}} \subset \sigma_r$.

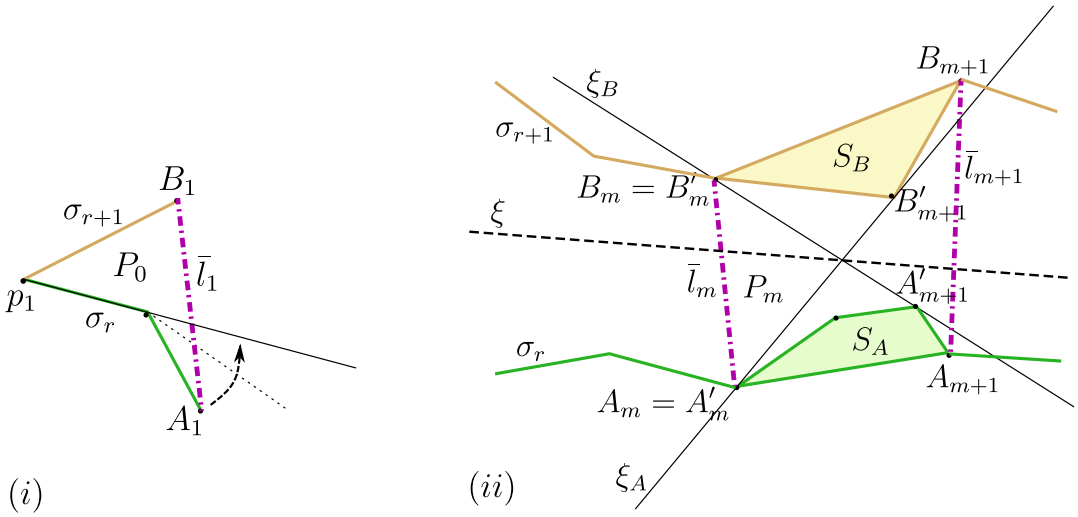

FIGURE 6.1. The folding patterns in the proof of Lemma 6.1: (i) corresponds to Step 1 and the interior polygon P_0 in Figure 5.4 (ii), the arrow indicates the direction of folding; (ii) corresponds to Step 2 and the polygon P_1 in Figure 5.4 (ii).

Since S_A and S_B are closed, convex and disjoint, there exist precisely two lines ξ_A, ξ_B which are supporting to both sets. Each of these lines intersects S_A and S_B either at a single vertex (which may be A_m or A_{m+1} for S_A and B_m or B_{m+1} for S_B) or along the whole segment which is the union of some consecutive edges in σ_r, σ_{r+1}. Denote $B'_m \in (\xi_A \cup \xi_B) \cap \sigma_{r+1}$ the vertex which is closest to B_m along σ_{r+1}, and let $B'_{m+1} \in (\xi_A \cup \xi_B) \cap \sigma_{r+1}$ be the vertex that is closest to B_{m+1} (along σ_{r+1}). Similarly, define $A'_m, A'_{m+1} \in (\xi_A \cup \xi_B) \cap \sigma_r$ as vertices on σ_r which are closest (possibly equal) to, respectively, A_m and A_{m+1} along σ_r.

Observe that ξ_A is precisely the line through A'_m and B'_{m+1} and that it intersects the closures of the cuts $\bar{l}_m$ and $\bar{l}_{m+1}$. By consecutive folding as in Step 1, one constructs an isometric immersion v of P_m with the property that its both boundary polygonal sides: from B_m to B_{m+1} and from A_m to A_{m+1} are mapped onto ξ_A. By a further rotation, we may ensure that $\xi_A = \mathbb{R}e_1$. Then:

$$v(B_m) - v(A_m) = \Big(- length(\overline{B_m \dots B'_{m+1}}) + length(\overline{A'_m B'_{m+1}}) + length(\overline{A_m \dots A'_m}) \Big) e_1 \doteq \alpha_v e_1.$$

Similarly, by folding on the line ξ_B through B'_m and A'_{m+1}, one obtains an isometric immersion w of P_m with both polygonal sides (namely, the sides distinct from $\bar{l}_m$ and $\bar{l}_{m+1}$) mapped on ξ_B. By a further rotation, we ensure that $\xi_B = \mathbb{R}e_1$, so that there holds:

$$w(B_m) - w(A_m) = \Big(- length(\overline{B_m \dots B'_m}) - length(\overline{A'_{m+1} B'_m}) + length(\overline{A_m \dots A'_{m+1}}) \Big) e_1 \doteq \alpha_w e_1.$$

Step 3. We now estimate the length of the vector $u(B_m) - u(A_m)$ that we need to achieve, and that is determined through previous steps in the construction. There clearly holds:

$$u(B_m) - u(A_m) = \Big(length(\overline{pa_{j_1} \dots B_m}) - length(\overline{pa_{i_1 \dots} A_m})\Big)e_1. \tag{6.1}$$

Since P_m contains no cuts in its interior, the polygonal: $\overline{pa_{i_1} \dots A_m A'_m B'_{m+1} B_{m+1} \dots a_{j_s} q}$ (this polygonal follows the portion of σ_r up to A'_m, then switches to σ_{r+1} along the segment $\overline{A'_m B'_{m+1}} \subset P_m$, and continues to q along σ_{r+1}) cannot be shorter than $length(\sigma_{r+1})$. Equivalently, we obtain:

$$\begin{aligned} &length(\overline{pa_{i_1} \dots A_m}) + length(\overline{A_m \dots A'_m}) + length(\overline{A'_m B'_{m+1}}) \\ &\quad \geq length(\overline{pa_{j_1} \dots B'_{m+1}}) = length(\overline{pa_{j_1} \dots B_m}) + length(\overline{B_m \dots B'_{m+1}}). \end{aligned}$$

By (6.1) the above yields:

$$\langle u(B_m) - u(A_m), e_1 \rangle \leq \alpha_v.$$

By a parallel argument, in which we concatenate σ_{r+1} up to B'_m with the segment $\overline{B'_m A'_{m+1}}$ and then with the portion of σ_r from A'_{m+1} to q, there follows the bound:

$$\begin{aligned} &length(\overline{pa_{j_1} \dots B_m}) + length(\overline{B_m \dots B'_m}) + length(\overline{B'_m A'_{m+1}}) \\ &\quad \geq length(\overline{pa_{i_1} \dots A_m}) + length(\overline{A_m \dots a'_{m+1}}), \end{aligned}$$

so (6.1) results in:

$$\langle u(B_m) - u(A_m), e_1 \rangle \geq \alpha_w.$$

Step 4. Let now ξ be any line passing through the intersection point $\xi_A \cap \xi_B$ and disjoint from the interiors of S_A and S_B (see Figure 6.1 (ii)). There exist exactly one line $\xi(A)$ which is supporting to the convex set S_A and parallel to ξ, and exactly one line $\xi(B)$ supporting to S_B and parallel to ξ. As before, we may fold the top portion of P_m so that the image of $\overline{B_m \dots B_{m+1}}$ is a segment within $\xi(B)$, and fold the bottom portion of P_m so that the image of $\overline{A_m \dots A_{m+1}}$ is a segment in $\xi(A)$. We now perform two more folds, which map both $\xi(A)$, $\xi(B)$ onto ξ, plus a rigid rotation that maps ξ onto $\mathbb{R}e_1$. Call the resulting isometric immersion u_ξ and observe that:

$$\text{the function } \ \xi \mapsto u_\xi(B_m) - u_\xi(A_m) \ \text{ is continuous.}$$

Since $u_{\xi_A} = v$ and $u_{\xi_B} = w$, the intermediate value theorem implies that $\langle u_\xi(B_m) - u_\xi(A_m), e_1 \rangle$ achieves an arbitrary value within the interval:

$$[\alpha_v, \alpha_w] = \Big[\langle u_{\xi_A}(B_m) - u_{\xi_A}(A_m), e_1 \rangle, \langle u_{\xi_B}(B_m) - u_{\xi_B}(A_m), e_1 \rangle\Big].$$

In conclusion, there exists a line ξ such that the corresponding u_ξ on P_m gives:

$$u_\xi(B_m) - u_\xi(A_m) = u(B_m) - u(A_m).$$

We set $u_{|P_m} \doteq u_\xi$.

Step 5. The final step is to construct u on P_s. This can be done by the same folding technique described in Step 1 for P_0. We then note that $\langle u(B_s) - u(A_s), e_1 \rangle$ automatically equals: $length(\overline{A_s \dots a_{j_l} q_1}) - length(\overline{B_s \dots a_{i_k} q_1})$, because $length(\sigma_r) = length(\sigma_{r+1})$. The proof is done. ■

7. Proof of Theorem 2.2, the general case. Step 3: isometric immersion on interior regions between and within consecutive trees

In this section we exhibit a procedure of constructing an isometric immersion on R_r, in the general setting (S1). Namely, we prove the following version of Lemma 6.1:

Lemma 7.1. *Assume (S), (S1) and fix $r = 1 \dots N-1$. Then, there exists a continuous, piecewise affine isometric immersion u of $R_r \setminus \bigcup_{m=1}^{s} T_m$ into $\mathbb{R}^3$, which satisfies:*

$$u(p) = 0, \quad u(q) = length(\sigma_1)e_1, \quad u(\sigma_r) = u(\sigma_{r+1}) = I.$$

Proof. We will inductively find the matching isometric immersions (always denoted by u) of the consecutive polygons in $P_0, \{Q_m \cup P_m\}_{m=1}^{s}$. Recall that we have defined two families of cut paths within each tree T_m: the path α_{m-1}^{right} joining vertices $A_{m-1}^{right} \in \sigma_r$ with $B_{m-1}^{right} \in \sigma_{r+1}$, and the path α_m^{left} joining vertices $A_m^{left} \in \sigma_r$ with $B_m^{right} \in \sigma_{r+1}$.

Step 1. Thus, the polygon P_0 is bounded by the the concatenation of: the portion of σ_{r+1} from p_1 to B_0^{right}, with α_0^{right}, with the portion of σ_r from A_0^{right} to p_1. We first fold the indicated portion of σ_{r+1} so that it coincides with the sub-interval:

$$\overline{length(\overline{pa_{i_1} \dots p_1})e_1, length(\overline{pa_{i_1} \dots B_0^{right}})e_1} \subset I.$$

This can be achieved as all internal angles of σ_{r+1} at vertices between p_1 and B_0^{right} are at least π. A symmetric folding can be done along the portion of σ_r within the boundary of P_0, see Figure 7.1 (i). This construction is similar to Step 1 in the proof of Lemma 6.1 (i).

As a result, the vector $u(B_0^{right}) - u(A_0^{right})$ equals $\big(length(\overline{pa_{i_1} \dots B_0^{right}}) - length(\overline{pa_{j_1} \dots A_0^{right}})\big)e_1$ and we consecutively have to find an isometric immersion of each region in the family Q_1, with the property that the vector $u(B_0^{right}) - u(A_0^{right})$ is prescribed, and that the images of the portion of σ_r between A_0^{right} and A_1^{left}, and of σ_{r+1} between B_0^{right} and B_1^{left}, are contained in $\mathbb{R}e_1$.

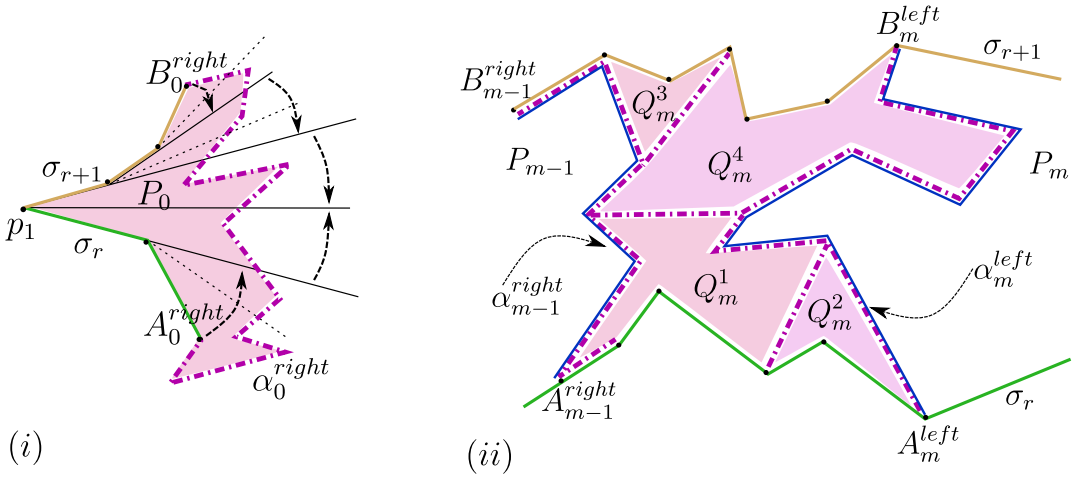

Figure 7.1. The folding patterns in the proof of Lemma 7.1: (i) corresponds to Step 1 and the polygon P_0, the arrows indicate the directions of folding; (ii) corresponds to Step 2 and the collection of polygons Q_m within the tree T_m.

Step 2. Assume that u has been constructed on $P_0 \cup Q_1 \cup \dots P_{m-1}$ for some $m \leq s$. Consider the tree T_m and the corresponding family of polygons Q_m enclosed between the paths of cuts α_{m-1}^{right}, α_m^{left} (both contained in T_m) and the portions of σ_r (respectively σ_{r+1}) between the vertices A_{m-1}^{right} and A_m^{left} (resp. B_{m-1}^{right} and B_m^{left}), see Figure 7.1 (ii). By Lemma 5.3 (iii), each polygon $Q_m^f \subset Q_m$ has an isometric immersion u in which the image of its boundary portion included in $\sigma_r \setminus T_m$ (or in $\sigma_{r+1} \setminus T_m$) is a segment on $\mathbb{R}e_1$. This construction consists of a collection of simple foldings as in Step 1 and Figure 7.1 (i), that can be implemented because all the internal (with respect to R_r) angles of Q_m^f at the vertices $\sigma_r \setminus T_m$ and $\sigma_{r+1} \setminus T_m$, are at least π.

Step 3. Assume that u has been constructed on $P_0 \cup Q_1 \cup \dots P_{m-1} \cup Q_m$ for some $m \leq s-1$. We now aim at describing u on the polygon P_m; note that the vector $u(B_m^{left}) - u(A_m^{left})$ is a prescribed, by the previous steps of the proof, scalar multiple of e_1. The construction below is based on the ideas of Steps 2-4 in the proof of Lemma 6.1, however the present setting of trees T replacing the single cuts $\bar{l}$ requires taking care of the additional details below.

Call ξ_A (respectively ξ_B) the shortest path in P_m that joins A_m^{left} with B_m^{right} (resp. A_m^{right} with B_m^{left}). We now estimate the length of the vector $u(B_m^{left}) - u(A_m^{left})$, namely:

$$\big\langle u(B_m^{left}) - u(A_m^{left}), e_1 \big\rangle = length(\overline{pa_{j_1} \dots B_m^{left}}) - length(\overline{pa_{i_1} \dots A_m^{left}}).$$

Since there are no cuts in the interior of P_m, it follows that the concatenation of the portion of σ_r from p to A_m^{left} with ξ_A and then with σ_{r+1} from B_m^{right} to q, cannot be shorter than σ_{r+1}. Equivalently:

$$length(\overline{pa_{i_1} \dots A_m^{left}}) + length(\xi_A) \geq length(\overline{pa_{j_1} \dots B_m^{right}}).$$

Also, concatenating σ_{r+1} up to B_m^{left} with ξ_B and then with the portion of σ_r from A_m^{right} to q, yields:

$$length(\overline{pa_{j_1} \dots B_m^{left}}) + length(\xi_B) \geq length(\overline{pa_{i_1} \dots A_m^{right}}).$$

The three last displayed bounds imply that:

$$\begin{aligned} &\big\langle u(B_m^{left}) - u(A_m^{left}), e_1 \big\rangle \in [\alpha_w, \alpha_v], \\ &\text{where } \ \alpha_v \doteq length(\xi_A) - length\big(B_m^{left} \dots (\sigma_{r+1}) \dots B_m^{right}\big), \\ &\qquad\quad \alpha_w \doteq length(\xi_B) - length\big(A_m^{left} \dots (\sigma_r) \dots A_m^{right}\big) \end{aligned} \tag{7.1}$$

Step 4. Since ξ_A has no self-intersections, it divides P_m into two connected components, and the endpoints B_m^{left}, A_m^{right} of ξ_B belong to the closures of the distinct components. Hence $\xi_A \cap \xi_B \neq \emptyset$.

Define C^{left} to be the vertex at which ξ_A detaches itself from σ_r (C^{left} may be equal to A_m^{left}) and C^{right} to be the vertex where ξ_B detaches from σ_r. Similarly, we have the detachment vertices $D^{left} \in \sigma_{r+1} \cap \xi_B$ and $D^{right} \in \sigma_{r+1} \cap \xi_A$. We observe in passing, that ξ_A and ξ_B used in the proof of Lemma 6.1 are precisely the portions of ξ_A, ξ_B that we use presently, between C^{left}, D^{right} and C^{right}, D^{left}. We now argue that C^{left} precedes or equals to C^{right} along σ_r (with the usual order from p to q). Assume by contradiction that C^{right} strictly precedes C^{left} and call γ the line spanned by the edge interval of σ_r that precedes C^{left}. By the minimizing length of ξ_A, its portion right after the detachment from σ_r stays in the half-plane S that is on the same side of γ as $\sigma_r \cap \partial P_m$.

Assume first that α_m^{left} has no intersection with ξ_A. In this case, ξ_A is the straight line from C^{left} up to D^{right}, and $\alpha_m^{right} \subset S$. Thus, α_m^{right} has no intersection with ξ_B and both ξ_B and α_m^{left} are contained in S, with ξ_B being a straight line from C^{right} to D^{left}. The fact that both $D^{left} \neq D^{right}$ are in $\sigma_{r+1} \cap S$ contradicts the concavity of $\sigma_{r+1} \cap \partial P_m$ and its disjointness from σ_r.

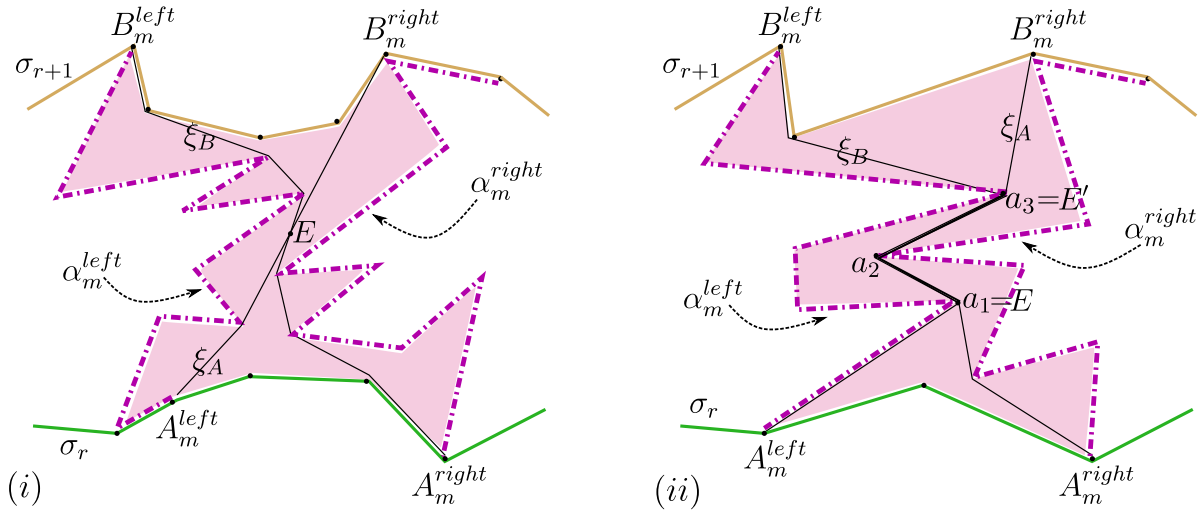

FIGURE 7.2. Two types of regions P_m (shaded) and the supporting polygonals ξ_A, ξ_B in the proof of Lemma 7.1 Step 4: in (i) the intersection $\xi_A \cap \xi_B$ consists of a single point E; in (ii) ξ_A and ξ_B intersect along the polygonal $\overline{a_1 a_2 a_3}$.

It hence follows that the polygonal ξ_A must have a common vertex with α_m^{left}. Let a be the first such vertex (in order from C^{left} to D^{right}; it necessarily belongs to S. Then D^{left} is contained in the region bounded by the concatenation of the portion of α_m^{left} from a to A_m^{left}, with σ_r from A_m^{left} to C^{left}, with the straight segment of ξ_A from C^{left} to a. Further, B_m^{right} cannot belong to the said region, unless $B_m^{right} = a$. This again contradicts the convexity of σ_{r+1} between D^{left} and B_m^{right}.

So indeed C^{left} (respectively D^{left}) precedes or equals C^{right} (resp. D^{right}) along σ_r (resp. σ_{r+1}).

Step 5. We now make further observation about the supporting polygonals ξ_A, ξ_B. Firstly, ξ_A (respectively ξ_B) have common vertices only with α_m^{left} (resp. α_m^{right}) from its endpoint on σ_r up to its first intersection point E with ξ_B (resp. ξ_A). Indeed, the first time that ξ_A encounters α_m^{right} it must also encounter ξ_B, and the first time ξ_B encounters α_m^{left} it must encounter ξ_A as well.

Secondly, the angles formed by ξ_A or ξ_B at these common vertices (up to E), interior with respect to the polygon with vertices C^{left}, E, C^{right} and with boundary along the appropriate portions of σ_r, ξ_A and ξ_B, are at least π. This fact is an easy consequence of ξ_A, ξ_B being shortest paths.

The two symmetric statements to those made above, are likewise valid for the portions of ξ_A, ξ_B from their endpoints on σ_{r+1} up to their respective first intersection point E' (there may be $E' = E$). Our last statement is that between E and E', the polygonals ξ_A, ξ_B coincide. For otherwise, ξ_A and ξ_B would be non-intersecting between some common vertices $\bar{E} \neq \bar{E}'$, hence bounding a polygon whose at least one angle other than $\bar{E}, \bar{E}'$ would be less than π (with respect to the polygon's interior). This would result in α_m^{left} or α_m^{right} having a vertex at the indicated angle, and hence necessarily intersecting the opposite boundary portion (of the polygon), which is a contradiction.

The two scenarios of $\xi_A \cap \xi_B$ consisting of a single intersection point, and of a polygonal with vertices in V (we recall that V is the set of vertices of the graph G) are presented in Figure 7.2.

Step 6. In this and the next Step we assume that:

$$E = E' \notin V. \tag{7.2}$$

We claim that there exists a folding pattern on P_m such that:

(i) the polygonal $\overline{C^{right}a_{h_1}\dots a_{h_z}D^{left}} \subset \xi_B$ has its image contained in some straight line $\bar{\xi}_B$,
(ii) the same polygonal has its image length unchanged from the original length,
(iii) the images of the portions of geodesics $\sigma_r \cap \partial P_m$, $\sigma_{r+1} \cap \partial P_m$ are their rigid motions.

For this construction, we write $E \in \overline{a_{h_t}a_{h_{t+1}}}$ and first consider the polygonal $\overline{Ea_{h_{t+1}}\dots a_{h_z}D^{left}}$ (see Figure 7.3 (i) with $t = 2$). We start at the vertex $a_{h_{t+1}}$ and perform the simple fold of the half-line that extends $\overline{a_{h_{t+1}}a_{h_{t+2}}}$ beyond $a_{h_{t+1}}$, intersected with P_m, onto the line spanned by the edge $\overline{a_{h_t}a_{h_{t+1}}}$. In doing so, we take advantage of the fact that both indicated lines intersect α_m^{right} before they may intersect σ_{r+1}. Next, we fold by bisecting the angle at the vertex $a_{h_{t+2}}$: the half-line extending $\overline{a_{h_{t+3}}a_{h_{t+2}}}$ beyond $a_{h_{t+2}}$ becomes the part of half-line that extends the (previously modified) segment $\overline{a_{h_{t+1}}a_{h_{t+2}}}$. We continue in this fashion, until we align $\overline{D^{left}a_{h_z}}$ with (previously modified) $\overline{a_{h_{z-1}}a_{h_z}}$. Similarly, we consider the polygonal $\overline{C^{right}a_{h_1}\dots a_{h_t}E}$, and starting from a_{h_t} we align $\overline{a_{h_t}a_{h_{t-1}}}$ with $\overline{a_{h_t}a_{h_{t+1}}}$. The final fold in this construction is that of half-line extending $\overline{C^{right}a_{h_1}}$ beyond a_{h_1}, intersected with P_m, onto the line spanned by $\overline{a_{h_1}a_{h_2}}$. As a result, the portion of ξ_B between C^{right} and D^{left} has been straightened onto the line $\bar{\xi}_B$ spanned by the segment $\overline{a_{h_t}a_{h_{t+1}}}$.

We now fold both portions of geodesics $\sigma_r \cap \partial P_m$ and $\sigma_{r+1} \cap \partial P_m$ onto $\bar{\xi}_B$, using their concavity, in the same manner as was done in the proof of Lemma 6.1 in the simplified context of section 6. By a further rotation we may exchange $\bar{\xi}_B$ into $\mathbb{R}e_1$ and denote the resulting isometric immersion of P_m by w. Recalling the notation in (7.1), it directly follows that:

$$w(B_m^{left}) - w(A_m^{left}) = \alpha_w e_1.$$

Similarly, by folding $(\sigma_r \cup \sigma_{r+1}) \cap \partial P_m$ onto the line $\bar{\xi}_A$ obtained as the straightening of the portion of ξ_A from C^{left} to D^{rigth}, we get an isometric immersion v of P_m with the property that:

$$v(B_m^{left}) - v(A_m^{left}) = \alpha_v e_1.$$

Step 7. Consider the family of lines $\{\xi\}$ obtained by rotating $\bar{\xi}_B$ around E onto $\bar{\xi}_A$. The direction of rotation (see Figure 7.3 (ii)) is so that the half-line from E through $a_{h_{t+1}}$ gets rotated onto the half-line from E to the vertex on ξ_A that is closest to E between E and C^{left}, without passing through D^{right} and C^{right} along the way. For each such line ξ we will describe the folding and the resulting isometry u_ξ on P_m, with the property that the function:

$$\xi \mapsto u_\xi(B_m^{left}) - u_\xi(A_m^{left})$$

is continuous and that $u_{\bar{\xi}_B} = w$, $u_{\bar{\xi}_A} = v$. By a further rotation, we may map ξ onto $\mathbb{R}e_1$ and hence conclude that the scalar function $\xi \mapsto \langle u_\xi(B_m^{left}) - u_\xi(A_m^{left}), e_1\rangle$ attains all values in the interval $[\alpha_w, \alpha_v]$. In virtue of (7.1), this will end the proof of Lemma 7.1 under the assumption (7.2).

Fix ξ as above and denote by ξ^1 the half-line emanating from E which is the rotated image of the half-line obtained by extending $\overline{Ea_{h_{t+1}}} \subset \bar{\xi}_B$ beyond $a_{h_{t+1}}$. We also denote $\xi^2 = \xi \setminus \xi^1$. Now, if ξ^1 intersects the portion of the polygonal ξ_B between E and D^{left} (we will refer to this intersection point by calling it a) , we utilize the same folding construction as in Step 6, but we replace the portion of ξ_B between E and a by the segment $\overline{Ea} \subset \xi$. Observe that $\overline{Ea}$ must intersect the boundary α_m^{left} of P_m before it reaches a. Thus there exists a simple fold which results in rotating (around a) of the edge of ξ_B containing a, onto ξ, and in such a way that the position of a remains unchanged, and that $\sigma_{r+1} \cap \partial P_m$ is also only transformed via a rigid motion. We then continue the straightening procedure of ξ_B beyond a as before.

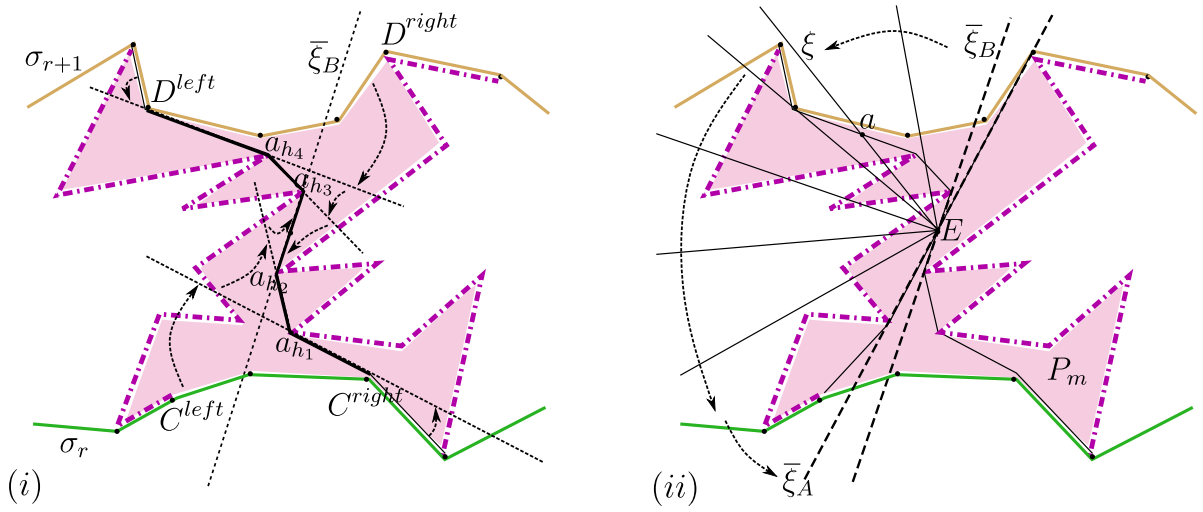

FIGURE 7.3. Elements of the proof of Lemma 7.1: diagram (i) depicts construction of the isometric immersion w on the region R_r as in Figure 7.2 (i). The arrows indicate the consecutive folds and the resulting straightenings of the intermediate polygonal $\overline{C^{right}a_{h_1}a_{h_2}a_{h_3}a_{h_4}D^{left}} \subset \xi_B$ to the line $\bar{\xi}_B$, and the projections of the boundary portions of σ_r, σ_{r+1} onto $\bar{\xi}_B$ in Step 6; diagram (ii) depicts the direction of rotating from $\bar{\xi}_B$ to $\bar{\xi}_A$, through the intermediate direction lines ξ in Step 7. The intersection point of the given half-line ξ^1 with the polygonal ξ_B is called a (provided it exists).

On the other hand, if the first intersection point a of ξ^1 with ξ_B occurs between D^{left} and B_m^{left}, we again take advantage of the fact that the open segment $\overline{Ea}$ must intersect α_m^{left}; this allows for a single simple fold which rotates the segment edge of ξ_B, to which a belongs (this edge must be contained in ξ_{r+1}) around a and onto ξ. In both so far described cases, the geodesic portion $\sigma_{r+1} \cap \partial P_m$ may be subsequently folded onto ξ, due to its concavity and the fact that its one point (D^{left} in the former case, a in the latter) already belongs to ξ^1.

In the third case when ξ^1 has no intersection with ξ_B beyond E (hence $\xi^1 \cap \sigma_{r+1} \cap \partial P_m = \emptyset$), we utilize the construction from proof of Lemma 6.1. This entails identifying the line γ that is parallel to ξ and supporting to $\sigma_{r+1} \cap \partial P_m$. We then first fold $\sigma_{r+1} \cap \partial P_m$ onto s, and then fold γ onto ξ. This, again, can be done without altering $\sigma_r \cap \partial P_m$ beyond possibly applying a rigid motion to it, because both lines ξ^2 and γ intersect α_m^{right} before they possibly intersect $\sigma_r \cap \partial P_m$.

Rotating ξ^1 further, we have it eventually pass through A_m^{left}, then C^{left}, then intersect the polygonal $\xi_A \setminus \sigma_r$, and finally coincide with the appropriate half-line in $\bar{\xi}_A$. In each of these listed scenarios, we perform the corresponding (in the reverse order of appearance) folding construction relative to the polygonal ξ_A rather than ξ_B. In the same fashion, we define the folding patterns relative to the half-line ξ^2. This concludes the definition of each u_ξ in case (7.2).

Step 8. Note that $E \neq E'$ implies $E, E' \in V$ (see Figure 7.2 (ii)). In this Step we assume that:

$$E = E' \in V \quad \text{or} \quad E \neq E'. \tag{7.3}$$

When $E \neq E'$, we first perform several simple folds which straighten the polygonal $\xi_A \cap \xi_B$ into a segment with endpoints that we continue to denote E and E', and such that the line spanned

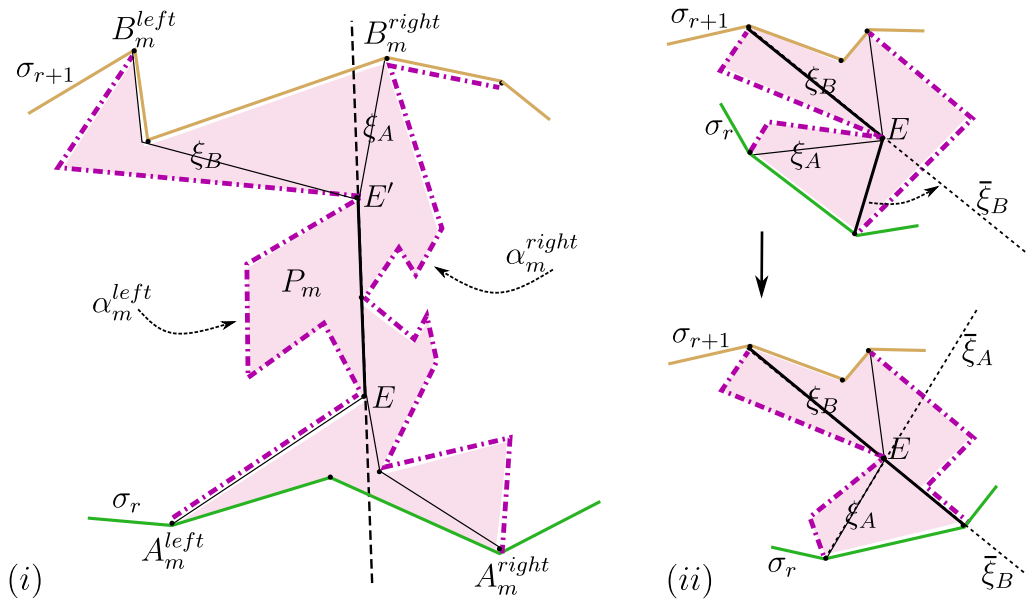

FIGURE 7.4. Construction in Step 8 of the proof of Lemma 7.1: (i) depicts the result of the initial folding, straightening $\xi_A \cap \xi_B$ into segment $\overline{EE'}$, applied to P_m in Figure 7.2 (ii); diagram (ii) indicates the initial folding in case $E = E'$.

by the new $\overline{EE'}$ enters each of the two angles between the pairs of distinct edges in ξ_A and ξ_B, emanating from E and E' (see Figure 7.4 (i)). As a result, the new polygonals ξ_A and ξ_B have the same convexity properties as in case (7.2). This allows for applying the folding construction in Step 7, relative to the center point $(E + E')/2$ and the projection lines $\bar{\xi}_B = \bar{\xi}_A$ spanned by $\overline{EE'}$.

When $E = E'$, we first perform one simple fold at the vertex E, which either: (i) makes the two edges of ξ_B with common vertex E collinear, and keeps the angle (internal to P_m) between the two edges of ξ_A adjacent to E not smaller than π; or (ii) makes the two edges of ξ_A with common vertex E collinear, and keeps the angle between the two edges of ξ_B adjacent to E not smaller than π. In what follows we will assume, without loss of generality, the former scenario as in Figure 7.4 (ii).

We let $\bar{\xi}_B$ to be the line spanned by the segment of ξ_B passing through E and $\bar{\xi}_A$ to be spanned by the segment with vertex E and the successive vertex along ξ_A towards C^{left}. We also call ξ_A^2 the half-line from E through the successive vertex along ξ_A towards D^{right}. We now apply the construction from Steps 6 and 7, where we rotate the line $\bar{\xi}_B$ onto $\bar{\xi}_A$ around E and perform a family of foldings onto each intermediate line ξ. In case $\xi_A^2 \not\subset \bar{\xi}_A$, the same construction is applied to each half-line emanating from E and intermediate to $\bar{\xi}_A$ and ξ_A^2, completed by an extra simple fold at E that aligns the said lines. This ends the definition of each u_ξ in case (7.3).

Step 9. The final step is to construct u on P_s. This can be done by the same folding technique as in Step 1. We also get: $\langle u(B_s^{left}) - u(A_s^{left}), e_1\rangle = length(\overline{A_s^{left} \dots a_{j_l} q_1}) - length(\overline{B_s^{left} \dots a_{i_k} q_1})$, because $length(\sigma_r) = length(\sigma_{r+1})$. This ends the proof of Lemma 7.1. ∎

8. Proof of Theorem 2.2. Step 4: isometric immersion on the exterior region. A counterexample when $p, q \notin \partial\Omega$

In this section, we first construct an isometric immersion u on the remaining region R_0.

Lemma 8.1. *Assume (S) and (S1). If $p, q \in \partial\Omega$ then there exists a continuous, piecewise affine isometric immersion u of R_0 into $\mathbb{R}^3$, satisfying:*

$$u(p) = 0, \quad u(q) = length(\sigma_1)e_1, \quad u(\sigma_1) = u(\sigma_N) = I.$$

Proof. By Lemma 5.2 we have: $R_0 \cap L = \emptyset$ and both the least and the greatest geodesics σ_1, σ_N are convex, i.e. the region $\Omega \setminus R_0$ has all the (internal) angles at the vertices distinct from p, q, not greater than π. Indeed, consider an intermediate vertex $A \notin \{p, q\}$ of σ_{min}. If the internal angle at A was strictly larger than π, then the cut $l = \overline{AB} \in E$ emanating from A would have to point inside R_0, as otherwise σ_{min} could be shortened, contradicting the fact that it is a geodesic. The argument for σ_{max} is similar. One can now apply the usual sequence of simple folds to obtain u on R_0. ∎

The proof of Theorem 2.2 is now complete. Note that the constructed isometric immersion u consists exclusively of planar folds and returns the image that is a subset of $\mathbb{R}^2$.

The fact that $R_0 \cap L = \emptyset$ is directly related to the assumption that $p, q \in \partial\Omega$. Indeed, examples in Figure 8.1 show there may be (even multiple) external trees, necessarily with vertices on both σ_1 and σ_N, when the said assumption is removed. This type of configuration may also be used to show that an isometric immersion u of $\Omega \setminus L$ with the property that the Euclidean distance between $u(p)$ and $u(q)$ equals the geodesic distance from p to q in $\Omega \setminus L$, may in general not exist.

Consider the example in Figure 8.2. It is easy to check that $\text{dist}_{\Omega\setminus L}(p, q) = c + 1 + \frac{1}{\sqrt{2}} = length(\sigma_1) = length(\sigma_2)$, when:

$$\alpha = \alpha(c) = \frac{1 - \frac{1}{\sqrt{2}} + (1 - \sqrt{2})c}{2c + 1}.$$

Also, the constraints $\frac{1}{\sqrt{2}} - c < \frac{1}{2}$ and $0 < \alpha < \frac{1}{2}$ (implying that the interior region R_1 has exactly the shape indicated in Figure 8.2) hold, in particular, when taking:

$$\frac{1}{\sqrt{2}} - \frac{1}{2} < c < \sqrt{2} - 1. \tag{8.1}$$

The minimality of the configuration $L = T_1 \cup T_2$ is guaranteed by requesting that: $length(\overline{pa_1pa_3q}) < \text{dist}(p, q)$, which upon a simple calculation reduces to: $c < \sqrt{2} - 1$, guaranteed in (8.1).

We now claim that there is no isometry u of $\Omega \setminus (T_1 \cup T_2)$, which straightens the polygonal $\overline{a_1a_2q}$. This is because otherwise there would be:

$$length(\overline{a_1a_2q}) = |u(q) - u(a_1)| \leq \text{dist}_{\Omega\setminus R_1}(a_1, q).$$

However, the inequality above is violated when the tree T_1 approximates closely the polygonal path $\overline{a_1pa_3q}$, in view of the bound $length(\overline{a_1pa_3q}) < length(\overline{a_1a_2q})$ which again follows from (8.1).

9. Discussion

Our two geometrical theorems are inspired by simple observations of the mechanical response of a sheet of paper that has cuts in it, valid only in the limit when the sheet is mapped to itself via a piecewise (non-unique) affine map that is isometric to the plane. To remove this non-uniqueness, we must account for the energetic penalty of deforming a sheet of small but finite thickness, by bending it out

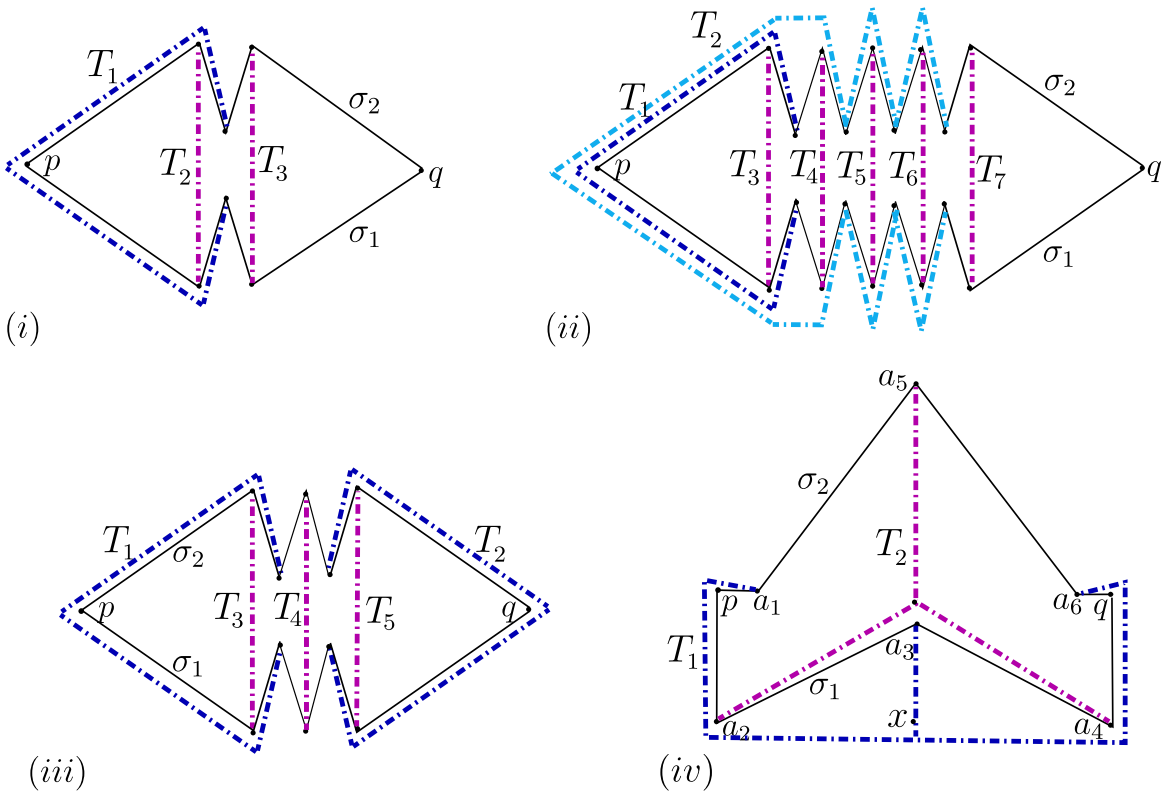

FIGURE 8.1. Examples of minimal configurations with the external region R_0 containing non-sealable cuts: in (i) the graph G consists of three trees $\{T_i\}_{i=1}^3$. There are two geodesics σ_1, σ_2 from p to q in $\Omega \setminus L$, a single internal region R_1 (which contains T_2, T_3) and the external region R_0 which contains T_1. Note that T_1 has leaves on both σ_1 and σ_2; in (ii) R_0 contains two "nested" trees T_1, T_2, while there are five more trees in R_1; in (iii) R_0 contains two trees T_1, T_2 (not "nested"); in (iv) we assume that $|\overline{pa_1}| < |\overline{a_2a_3}| - |\overline{a_2x}|$, for minimality. There is a single tree T_1 in R_0 and a single tree T_2 in R_1. The two geodesics are: $\sigma_1 = \overline{pa_2a_3a_4q}$ and $\sigma_2 = \overline{pa_1a_5a_6q}$.

of the plane. When this physical fact is accounted for, a kirigamized sheet will deform into a complex shape constituted of conical and cylindrical structures glued together. A combination of physical and numerical experiments can be used to characterize the geometric mechanics of kirigamized sheets as a function of the number, size, and orientation of cuts. This is the topic of a complementary study [12], which in particular shows that by varying the geodesic lengths, one can shape the deployment trajectory of a sheet as well as control its compliance across orders of magnitude in the force.

Understanding the mechanics and mathematics of these objects, while also solving the inverse problem of how to design the number, size, orientation and location of the cuts, remain open problems. And while we have limited ourselves to the study of Euclidean case, our study naturally raises questions about the nature and form of geodesics in non-Euclidean surfaces with co-dimension one obstructions, and higher-dimensional generalizations that might be relevant for traffic, fluid flow and stress transmission in continuous and discrete geometries.

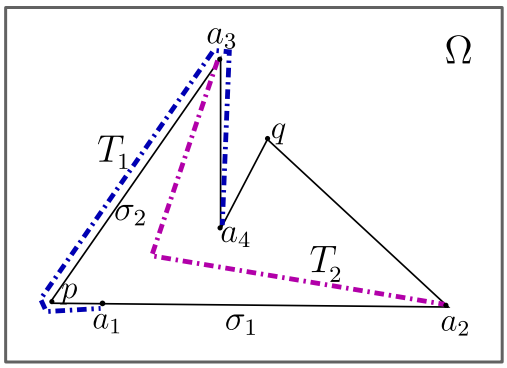

FIGURE 8.2. A configuration of G, Ω and $p, q \in \Omega$ for which the conclusion of Theorem 2.1 fails. The set of vertices of G is: $V = \{a_1 = (0,0), a_2 = (1,0), a_3 = (\frac{1}{\sqrt{2}} - c, \frac{1}{\sqrt{2}}), a_4 = (\frac{1}{\sqrt{2}} - c, \alpha)\}$ and $p = (-c, 0), q = (\frac{1}{2}, \frac{1}{2})$. The set of cuts is: $L = T_1 \cup T_2$, where T_1 is the single exterior tree and T_2 is the single interior tree. For every $\frac{1}{\sqrt{2}} - \frac{1}{2} < c < \frac{1}{\sqrt{2}}$ there exists $0 < \alpha < \frac{1}{2}$ so that there are two geodesics $\sigma_1 = \overline{pa_1a_2q}$, $\sigma_2 = \overline{pa_3a_4q}$ satisfying: $length(\sigma_1) = length(\sigma_2) = 1 + \frac{1}{\sqrt{2}} + c$. When additionally $c < \sqrt{2} - 1$, then the above configuration is minimal.

REFERENCES

[1] Bertoldi, K., Vitelli, V., Christensen, J. and Van Hecke, M., 2017. *Flexible mechanical metamaterials.* Nature Reviews Materials 2(11), pp. 1-11.

[2] Blees, M.K., Barnard, A.W., Rose, P.A., Roberts, S.P., McGill, K.L., Huang, P.Y., Ruyack, A.R., Kevek, J.W., Kobrin, B., Muller, D.A. and McEuen, P.L., 2015. *Graphene kirigami.* Nature, 524(7564), pp. 204-207.

[3] Callens, S. and Zadpoor, A., 2018. *From flat sheets to curved geometries: Origami and kirigami approaches.* Materials Today 21.3, pp. 241-264.

[4] Conti, S., De Lellis, C., Székelyhidi Jr., L., *h-principle and rigidity for $c^{1,\alpha}$ isometric embeddings*, Proceedings of the Abel Symposium, 2010.

[5] Cao, W., Székelyhidi Jr., L., *Global Nash-Kuiper theorem for compact manifolds.* J. Diff. Geom., to appear. ArXiv preprint:1906.08608v2.

[6] De Lellis, C., Inauen, D., Székelyhidi Jr., L., *A Nash-Kuiper theorem for $C^{1,1/5-\delta}$ immersions on surfaces in 3 dimensions*, Rev. Mat. Iberoamericana, 34(2018), 1119-1152.

[7] Demaine ED, O'Rourke J. *Geometric folding algorithms: linkages, origami, polyhedra.* Cambridge university press; 2007.

[8] Hull TC. *Origametry: Mathematical Methods in Paper Folding.* Cambridge University Press; 2020.

[9] Storer, James A., and John H. Reif. *Shortest paths in the plane with polygonal obstacles* Journal of the ACM (JACM) 41, no. 5: 982-1012, 1994.

[10] Sharir M, Schorr A. *On shortest paths in polyhedral spaces* SIAM Journal on Computing; 15(1):193-215, 1986.

[11] Polthier, Konrad and Schmies, Markus, *Straightest geodesics on polyhedral surfaces*, ACM SIGGRAPH 2006 Courses, 30–38, 2006

[12] Chaudhary, G., Niu, L., Lewicka, M., Han, Q. and Mahadevan, L., 2021. *Geometric mechanics of random kirigami.* ArXiv preprint: .

[13] Günther, M., *Zum Einbettungssatz von J. Nash.* Math. Nachr., 144(1989), 165-187.

[14] Han, Q., Hong, J.-X., *Isometric Embedding of Riemannian Manifolds in Euclidean Spaces*, Mathematical Surveys and Monographs, Volume 130, American Mathematical Society, Providence, RI, 2006.

[15] Choi, GP., Dudte, LH. and Mahadevan, L., 2019. *Programming shape using kirigami tesselations.* Nat. Materials 18, pp. 999-1004.

[16] Choi, GP., Dudte, LH. and Mahadevan, L., 2020. *Compact reconfigurable kirigami.* ArXiv:2012.09241.

[17] Kuiper, N., *On C^1 isometric embeddings I, II.* Proc. Kon. Acad. Wet. Amsterdam A, 58(1955), 545-556, 683-689.
[18] Nash, J., *C^1 isometric imbeddings.* Ann. Math., 60(1954), 383-396.
[19] Nash, J., *The embedding problem for Riemannian manifolds*, Ann. of Math., 63(1956), 20-63.
[20] Rafsanjani, A. and Bertoldi, K., 2017. *Buckling-induced kirigami.* Physical Review Letters, 118(8), p. 084301.

Qing Han: Department of Mathematics, University of Notre Dame, Notre Dame, IN 46556

Marta Lewicka: University of Pittsburgh, Department of Mathematics, 139 University Place, Pittsburgh, PA 15260

L. Mahadevan: Harvard University, School of Engineering and Applied Sciences, and Department of Physics, 29 Oxford Street, Cambridge, MA 02138
E-mail address: Qing.Han.7@nd.edu, lewicka@pitt.edu, lmahadev@g.harvard.edu